ISET Journal of Earthquake Technology, Paper No. 416, Vol. 39, No. 1-2, March-June 2002, pp. 21-53

ENERGY OF EARTHQUAKE RESPONSE – RECENT DEVELOPMENTS

Tzong-Ying Hao
Department of Civil Engineering, University of Southern California
Los Angeles, CA 90089-2531, U.S.A.

ABSTRACT

This paper reviews research related to energy methods for earthquake-resistant design of structures, with an emphasis on the most recent developments, which for the first time consider all the stages of the seismic energy flow, starting from the earthquake source, and including the effects of the soil-structure interaction. Results are presented for five case studies (four reinforced concrete buildings and one steel structure). For these buildings, the correspondence between the total incident wave energy and the sum of all energies associated with the response of their soil-structure systems is analyzed. Some elementary aspects of design, based on the power of the incident wave pulses, are discussed. It is shown how this power can be compared with the capacity of the structure to absorb the incident wave energy. The advantages of using the computed power of incident strong motion to design a structure for linear or for partially destructive relative response are discussed.

KEYWORDS: Flow of Earthquake Energy, Non-linear Soil Response, Soil-Structure Interaction, Energy Absorption Capacity, Earthquake Resistant Design

INTRODUCTION

1. General

Spatial distributions of earthquake damage are far too complicated and can change over so short distances (Trifunac and Todorovska, 1997a, 1997b, 1998a, 1998b, 1998c, 1998d, 1999) that it is not possible, at present, to associate those with same amplitude characteristics of recorded motions. The most densely instrumented metropolitan areas still have too sparse distributions of strong motion accelerographs (e.g., Trifunac and Todorovska, 2001) to help identify the principal causes of damage. Numerous empirical correlations of the degree of damage versus simple indicators of the severity of strong motion (e.g., peak velocity, site intensity) have been published, but only limited results exist on the use of energy and power of incident strong motion waves. Before such correlations are initiated, it seems appropriate to review the details of energy flow through a soil-foundation-structure system, so that the nature of motion leading to damage, geographically, and within a structure may be understood (Trifunac and Hao, 2001; Trifunac et al., 1999b, 2001d, 2001e).

Traditionally, displacement ductility has been used as a criterion for earthquake-resistant design of structures. Alternative energy-related concepts were discussed by Benioff (1934), Sezawa and Kanai (1936), Tanabashi (1937), and later by Tanabashi (1956), Housner (1956) and Blume (1960). Figure 1 outlines the milestones of the work on earthquake-resistant design, the years of the significant earthquakes (from earthquake engineering point of view), and the years of the World Conferences on Earthquake Engineering.

In 1934, Benioff proposed a measure of seismic destructiveness to be computed via the area under the relative displacement response spectrum. It can be shown that this result can be related to the energy of response to strong motion (Arias, 1970; Trifunac and Brady, 1975). Benioff did not discuss strong motion energy explicitly. However, his definition of destructiveness as "the integral with respect to pendulum frequency of the maximum displacement of an infinite series of undamped pendulums" is directly related to the energy of response.

The current seismic design codes describe the earthquake excitation as an acceleration response spectrum, which prescribes the required horizontal loads representing a design earthquake. An acceleration response spectrum displays the maximum absolute acceleration response, and its shape reflects the frequency content of the excitation (Biot, 1932, 1933, 1934, 1941, 1942). Although the acceleration response spectra provide a convenient tool for quantifying an earthquake input, research

indicates that this is not sufficient for expressing the damage potential of earthquake ground motion. The seismic energy input, and the seismic energy dissipation during strong shaking, can represent the damage potential of an earthquake ground motion more directly than spectral acceleration.

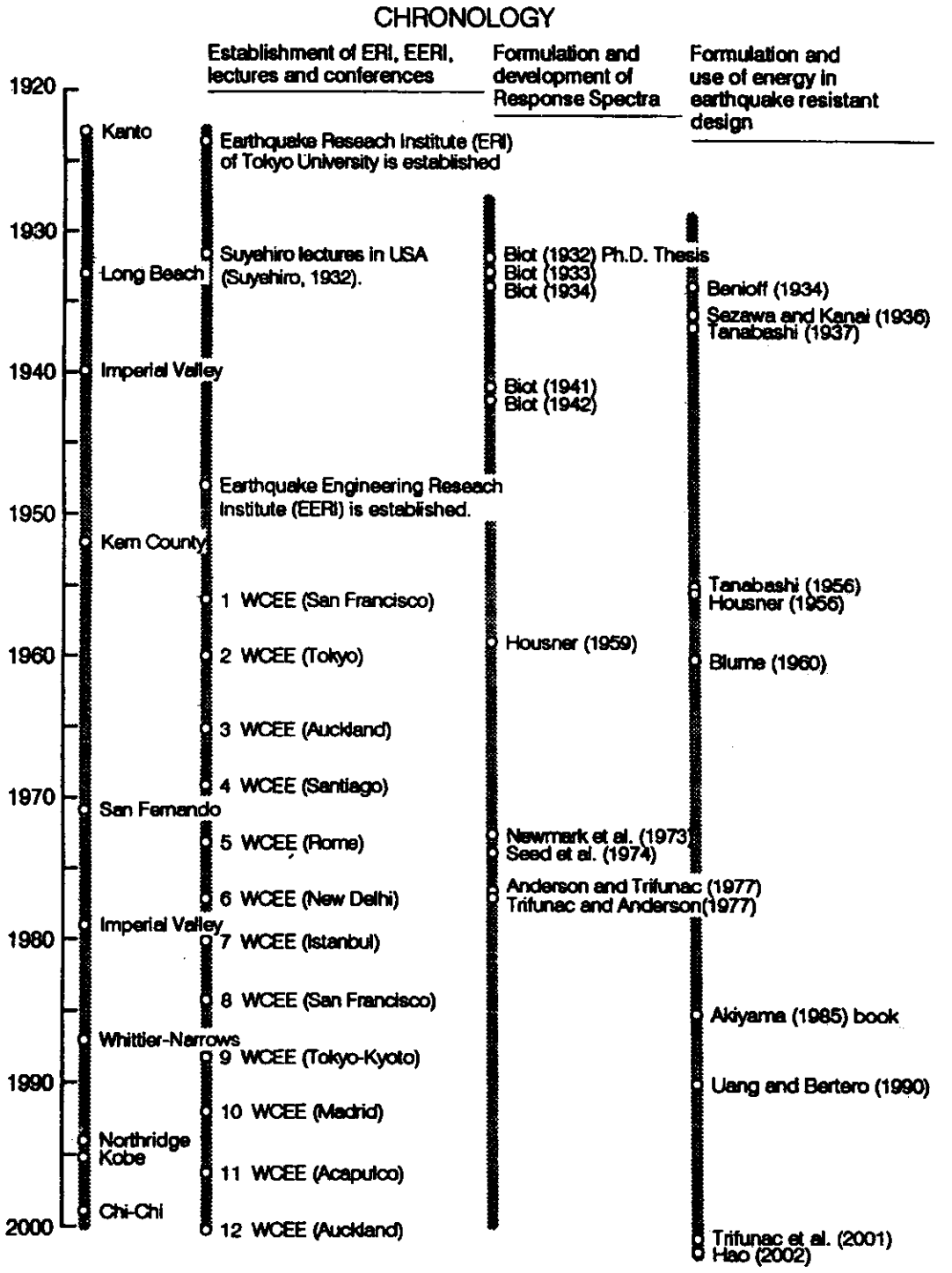

Fig. 1 Historical milestones in Earthquake Engineering, with emphasis on the subject of earthquake-resistant design (the years of selected significant earthquakes (from earthquake engineering point of view) and of the World Conferences on Earthquake Engineering are marked)

In this paper, we review an alternative to the spectral method of earthquake-resistant design by analyzing the flow of energy associated with strong motion, and by focusing on the energy during soil-foundation-structure system response. In Figure 2, the principal stages of the earthquake wave energy flow, from the earthquake source, along the propagation path, and finally to the work leading to relative response of the structure, are outlined. The losses of energy at every stage are also outlined. These losses must be accounted for to accurately quantify the remaining energy that will excite the structure.

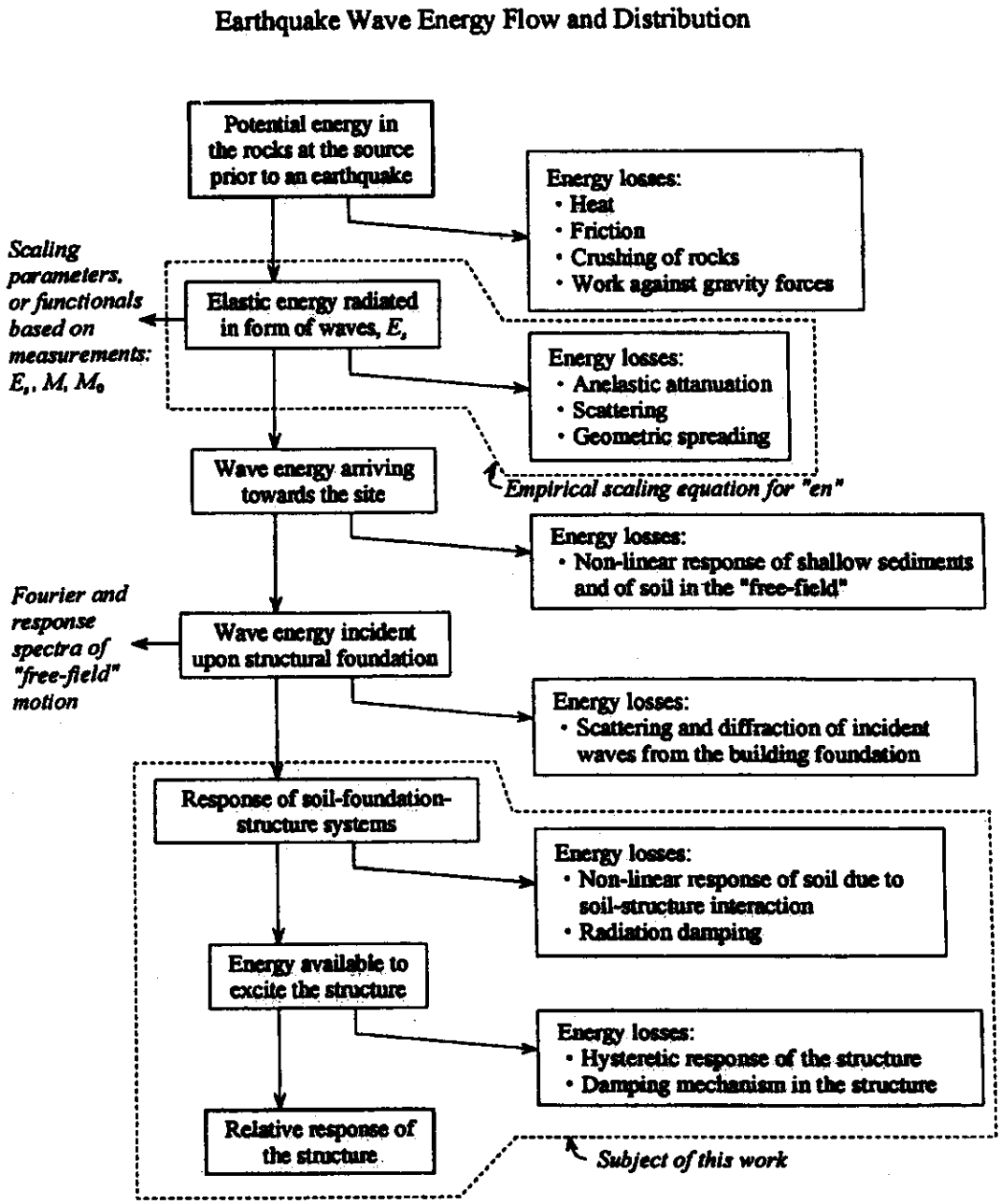

Fig. 2 An outline of the principal stages in the flow of earthquake wave energy from the earthquake source to a structure

2. Literature Review and Key Issues on Energy in Structural Response

The formulation of a rational design approach based on energy concepts requires understanding of the effects of the incident energy and other relevant parameters external to the structure (e.g., earthquake magnitude, distance to the causative fault) on the response of earthquake-resistant structures.

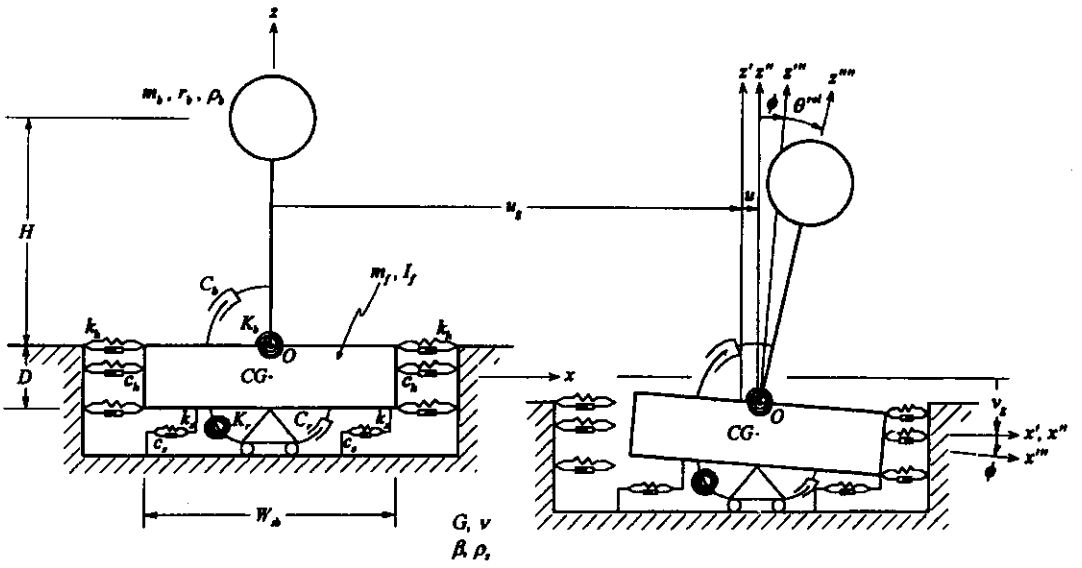

Fig. 3 A model of a soil-foundation-building system in an undeformed (left) and a deformed (right) configuration

The energy associated with the elastic waves radiated from the earthquake source, E_s (Gutenberg and Richter, 1956), is attenuated with increasing epicentral distance, R, through the mechanisms of inelastic attenuation, scattering, and geometric spreading (Trifunac, 1994; Trifunac et al., 2001f). The earthquake wave energy arriving towards the site is next dissipated by non-linear response of the shallow sediments and soil in the free-field (Joyner, 1975; Joyner and Chen, 1975; Trifunac, 1995; Trifunac and Todorovska, 1996, 1998), before it begins to excite the foundation. Once the foundation is excited by the incident earthquake waves, the response of the soil-structure system is initiated. The available incident wave energy is reduced by non-linear deformation of the soil during soil-structure interaction (Trifunac et al., 1999a, 2001a, 2001b) and by radiation damping (Luco et al., 1986; Rodrigues and Montes, 2000; Todorovska and Trifunac, 1991). The earthquake wave energy flow and distribution involving the last three stages in Fig. 2: (1) the response of the soil-foundation-structure system, (2) the energy available to excite the structure, and (3) the relative response of the structure, will be reviewed in this work.

The total energy input into a structure exerted by an earthquake depends mainly on the total mass and on the fundamental natural period of the structure (Akiyama, 1985, 1988, 1997; Uang and Bertero, 1988). Energy dissipation, as a means of reducing the seismic response of structures, has become also an important topic among the designers who develop friction dampers, fluid dampers, and isolators.

A natural form of energy dissipation occurs during interaction between a structure, its foundation, and the supporting soil medium. This dissipated energy can be significant and will contribute towards reduction of the seismic response. Unfortunately, this energy sink is often disregarded by researchers and engineers. Moreover, most modern structures are designed to resist severe loading conditions for which inelastic action exists only in the superstructure response. Hence, there is a need to develop soil-foundation analysis models which can account for inelastic behavior of the soil. The non-linearity can occur either in the superstructure, in the foundation, in the supporting soil medium, or in all of those simultaneously. Consequently, a good and realistic model must have features describing the response of the soil-foundation-structure system as completely and as accurately as possible.

For the majority of structures, inelastic behavior is accepted in the design for severe earthquake shaking. The effects of such inelastic behavior on the intensity and spectral distribution of the energy demands were investigated by Rodrigues and Montes (2000) and Decanini and Mollaioli (2001). Fajfar and Fischinger (1990), Uang and Bertero (1990), and Tembulkar and Nau (1987) evaluated the effect of non-linear behavior on the seismic input energy of SDOF systems. Zahrah and Hall (1984) evaluated the non-linear response of simple structures and the damage potential of an earthquake ground motion, as measured in terms of the amount of energy imparted to a structure, the amount of energy dissipated by inelastic deformation and by damping, as well as by the assessment of the displacement ductility of the

structure and the number of yielding excursions and reversals experienced during the excitation. Uang and Bertero (1988) discussed the derivation of the two "energy equations" (absolute and relative), and showed that the maximum values of the absolute and relative energy input, E_I, for any given constant displacement ductility ratio are very close in the period range of practical interest for earthquake-resistant design of buildings (0.3 to 5.0 seconds).

In most published studies, the derivation of energy equations begins by integrating the differential equation of dynamic equilibrium of a single-degree-of-freedom system with respect to displacement, which results in

$$E_I = E_E + E_D = E_K + E_S + E_{H\xi} + E_{H\mu} \quad (1)$$

where E_I is the energy input, E_E is the stored elastic energy, E_D is the dissipated energy through viscous-damping mechanisms, E_K is the kinetic energy, E_S is the elastic strain energy, $E_{H\xi}$ is the energy dissipated through hysteretic damping, and $E_{H\mu}$ is the energy dissipated by the hysteretic plastic deformation.

An important omission in many of the published studies is that the effects of soil-structure interaction are ignored. Because of that, significant energy loss mechanisms (non-linear response of the soil and radiation damping) are neglected (Figure 2; see also Rodrigues and Montes, 2000). The other extreme is to neglect the stiffness of the foundation system (and the soil-structure interaction), and to assume that the wave energy in the soil drives the building to follow the motions specified by the wave propagation in the free-field. This approximate approach underestimates the scattering of incident wave energy by the foundation and overestimates the energy transmitted into the building. The reality is somewhere between these two extremes, and can be studied further in detail only by numerical methods. Other simplifications and omissions in Equation (1) are that the dynamic instability and the effects of gravity on non-linear response are ignored (Husid, 1967; Lee, 1979; Todorovska and Trifunac, 1991, 1993).

At present, the model most commonly used by engineers for the design of buildings assumes the structure to be fixed to a "rigid" ground. Current design methods thus disregard the influence that the flexibility of the ground has on the response of a structure. Such a procedure simplifies the analysis. The assumption that there is no coupling or interaction between the structure, its foundation and the supporting soil is however contrary to recorded observations (Trifunac et al., 1999a; 2001a, 2001b). The conceptual model proposed by Trifunac et al. (2001f) and Hao (2002) attempts to capture the main characteristics of the non-linear behavior of soil-structure systems, and will be described in the following.

ENERGY DURING SOIL-FOUNDATION-STRUCTURE SYSTEM RESPONSE

1. Model

To describe the energy flow through a soil-foundation-structure system, Hao (2002) and Trifunac et al. (2001f) use the idealized mathematical model shown in Figure 3. In this model, the building is represented by an equivalent single-degree-of-freedom (SDOF) oscillator founded on a rigid embedded rectangular foundation. The soil has shear modulus G, shear wave velocity β, Poisson's ratio ν, and mass density ρ_s. The oscillator has only one degree-of-freedom with respect to the foundation, θ^{rel}. The mass of the oscillator is m_b. It has height H and radius of gyration r_b. The oscillator is connected to the foundation at point O through a rotational spring and a viscous damper. The spring has stiffness K_b, and the viscous damper has damping constant C_b. The stiffness is chosen such that the natural period of the oscillator, T_1, is equal to the corresponding fixed-base period of the fundamental mode of the building. Assuming that the equivalent SDOF oscillator has same mass per unit length as the real building, assumed to deform in shear only, H and r_b are related to H_{sb} and W_{sb}, the height and width of the real building (Todorovska and Trifunac, 1993), as $H = H_{sb}/\sqrt{3}$ and $r_b = W_{sb}/\sqrt{3}$.

The rectangular foundation has width W_{sb}, depth D, mass m_f, and mass moment of inertia I_f. To simplify the analysis, Hao (2002) and Trifunac et al. (2001f) assume that the stiffness of the soil in the vertical direction is infinite. The foundation has two degrees-of-freedom with respect to its center of

gravity (point *CG*): horizontal translation, u, and rotation, ϕ. The foundation is surrounded by springs and dashpots, which model the reactive forces caused by deformation developed in the soil (Richart et al., 1970). In Figure 3, k_h and c_h are the stiffness and damping constants of horizontal springs and dashpots around the foundation representing the horizontal reactive forces on the vertical faces of the foundation; k_z and c_z are the stiffness and damping constants of the horizontal springs and dashpots at the base of the foundation representing the shear forces acting on the interface; and K_r and C_r are the rotational stiffness and damping constant representing the resisting moments in the half-space. The evaluation of the stiffness $(k_h,\ k_z \text{ and } K_r)$ and damping $(c_h,\ c_z \text{ and } C_r)$ constants is discussed in Trifunac et al. (2001f). This soil-foundation-oscillator system is subjected to horizontal and vertical excitations $(u_g \text{ and } v_g)$.

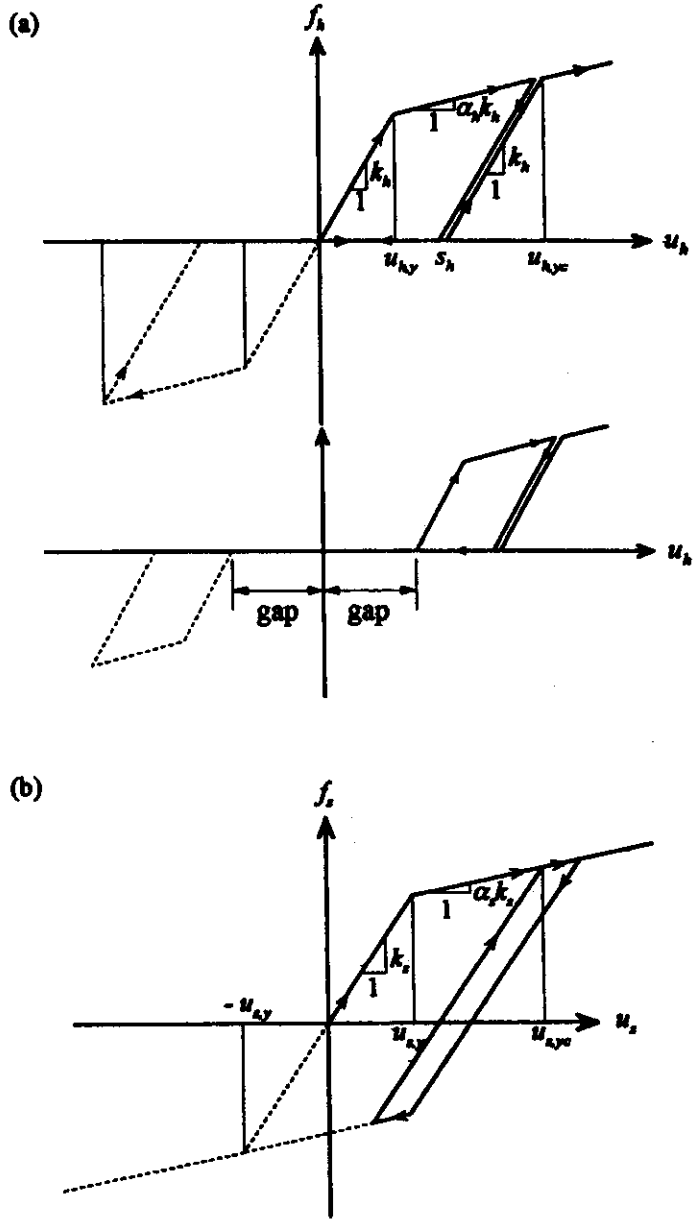

Fig. 4 Force-deformation relations used to represent the nonlinear behavior of soil: (a) slip model for horizontal springs on two sides of the foundation, (b) bilinear model for springs at the base of the foundation

Hao (2002) and Trifunac et al. (2001f) further assume that the foundation is rigid, in order to reduce the number of degrees-of-freedom of the model (Duncan, 1952; Trifunac and Todorovska, 2001). Such models give an approximation of the system response for long wavelengths relative to the foundation dimensions (Lee, 1979). For short wavelengths, this assumption can result in nonconservative estimates of the relative deformations in the structure (Trifunac, 1997; Trifunac and Todorovska, 1997), and, in general, is expected to result in excessive estimates of scattering of the incident wave energy and in excessive radiation damping (Todorovska and Trifunac, 1990a, 1990b, 1990c, 1991, 1992, 1993). The extent to which this simplifying assumption is valid, depends on the stiffness of the foundation system relative to that of the soil, and also on the overall rigidity of the structure (Iguchi and Luco, 1982; Liou and Huang, 1994; Hayir et al., 2001; Todorovska et al., 2001a, 2001b, 2001c; Trifunac et al., 1999a).

Ivanović et al. (2000) and Trifunac et al. (2001a, 2001b, 2001c) suggested that the soil behavior is non-linear during most earthquakes, and that it can recover its stiffness after consolidation with time, and after small amplitude shaking from aftershocks and smaller earthquakes. The observed "softening" and "hardening" behavior of the system can be explained by a model with *gap* elements along the contact between the foundation and the soil. We can assume that the soil on the side of the foundation is represented by a hysteretic slip model (see Figure 4(a)) to simulate the non-linear behavior of the soil. This slip model emphasizes the pinching effects of soil with large stresses and the *gap* generated by soil compression. For the soil at the base of the foundation, the bilinear and softening characteristics are represented in Figure 4(b). A detailed description of these slip and bilinear hysteretic systems is presented in Trifunac et al. (2001f).

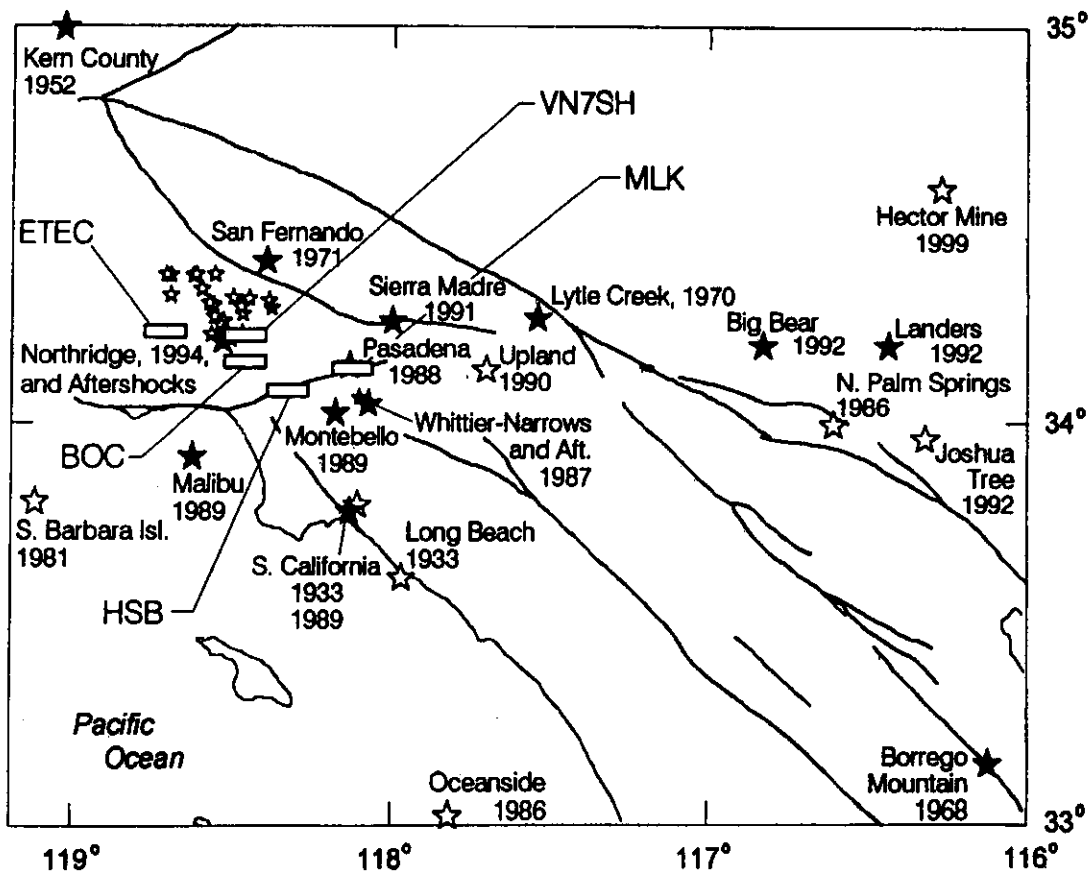

Fig. 5 Earthquakes in Southern California, large enough to trigger the strong motion accelerographs in HSB, VN7SH, BOC, MLK and ETEC (the rectangles indicate the five buildings being studied; the events for which strong motion data was recorded and is available in digitized form can be found in Hao, 2002)

2. Equations of Motion

The equations of motion for the system are derived and solved including the non-linear geometry and soil behavior, coupling of the vertical acceleration with the rocking and horizontal translation, and the effects of the gravity forces $(m_b g$ and $m_f g)$. It is not required to assume small deformations assumption, and arbitrary material non-linearity is allowed. The response of the building and of the soil can enter inelastic range during strong ground shaking. In that case, the analysis of soil-structure interaction (SSI) will be quite complicated. Consequently, at first, the building will be assumed to be linear, and the soil will be assumed to exhibit inelastic force-deformation relation. Later on, we will briefly consider the non-linear response of the building also.

The equations of motion for the system then can be derived from the equilibrium of forces and moments. From the equations of dynamic equilibrium of forces in the horizontal and vertical directions and all moments acting on the oscillator about point O, the interactive forces and the moment between the oscillator and foundation are

$$\Sigma F_x = 0 \Rightarrow f_{x,b} = m_b \ddot{u}_b \tag{2}$$

$$\Sigma F_z = 0 \Rightarrow f_{z,b} = -m_b(\ddot{v}_b - g) \tag{3}$$

$$\begin{aligned}\Sigma M_O = 0 \Rightarrow & I_O(\ddot{\phi} + \ddot{\theta}^{rel}) + m_b \ddot{u}_O H\cos(\phi + \theta^{rel}) + m_b(\ddot{v}_O - g)H\sin(\phi + \theta^{rel}) \\ & + K_b\theta^{rel} + C_b\dot{\theta}^{rel} = 0\end{aligned} \tag{4}$$

where $I_O = m_b r_b^2[1 + (\frac{r_b}{H})^2]$.

From the equations of dynamic equilibrium of all forces and moments acting on the foundation about point CG, it follows that

$$\Sigma F_x = 0 \Rightarrow \sum_{i=1}^{m} f_{h,i} + \sum_{j=1}^{n} f_{s,j} = -m_f \ddot{u}_{CG} - f_{x,b} \tag{5}$$

$$\Sigma F_z = 0 \Rightarrow f_{z,f} = -m_f(\ddot{v}_{CG} - g) + f_{z,b} \tag{6}$$

$$\begin{aligned}\Sigma M_{CG} = 0 \Rightarrow M_{B,f} = & (f_{z,b} + f_{z,f})\frac{D}{2}\sin\phi - f_{x,b}\frac{D}{2}\cos\phi + M_{O,b} - I_f\ddot{\phi} \\ & - \sum_{i=1}^{m}(f_{h,i}\cos\phi)d_i + \sum_{i=1}^{m}(f_{h,i}\sin\phi)\frac{W_{sb}}{2} - \sum_{j=1}^{n}(f_{s,j}\sin\phi)l_i + \sum_{j=1}^{n}(f_{s,j}\cos\phi)\frac{D}{2}\end{aligned} \tag{7}$$

and

$$M_{B,f} = K_r\phi + C_r\dot{\phi}. \tag{8}$$

3. Derivation of the Energy Equations

When a system is subjected to earthquake shaking, the incident waves propagate into it. During strong ground motion, part of the incident energy is dissipated by scattering from the foundation and by the deformation of the soil, and the rest is transmitted into the building.

Referring to the model in Figure 3, all forces and moments move through the corresponding displacements and thus do work. To evaluate this work, we integrate all six equilibrium equations of the system, Equations (2), (3), (4), (5), (6) and (7), with respect to the corresponding displacements. The total work done in the system is then computed by superposition of integrals of those equations.

To simplify these energy formulae, we keep only the first order terms of the Taylor series expansions of the sine and cosine functions of the angles θ^{rel} and ϕ (and their linear combination), and eliminate the products of small angles and of their derivatives. Then, the above six equations give

$$\int\{m_b[\ddot{u} + \frac{D}{2}\ddot{\phi} + H(\ddot{\phi} + \ddot{\theta}^{rel})] - f_{x,b}\}\,\dot{u}_b\,dt = -\int m_b \ddot{u}_g \dot{u}_b dt \tag{9}$$

$$\int(-m_b g + f_{z,b})\,\dot{v}_b\,dt = -\int m_b \ddot{v}_g \dot{v}_b\,dt \tag{10}$$

$$\int[m_b(\ddot{u}_O + \frac{D}{2}\ddot{\phi})H - m_b g H\phi_b + I_O\ddot{\phi}_b + K_b\theta^{rel} + C_b\dot{\theta}^{rel}]\,\dot{\phi}_b\,dt = -\int(m_b\ddot{u}_g H + m_b\ddot{v}_g H\phi_b)\,\dot{\phi}_b\,dt \tag{11}$$

$$\int(m_f\ddot{u} + f_{x,b})\,\dot{u}_{CG}\,dt + \int(\sum_{i=1}^{m} f_{h,i} + \sum_{j=1}^{n} f_{s,j})\,\dot{u}\,dt = -\int m_f\ddot{u}_g\dot{u}_{CG}\,dt \tag{12}$$

$$\int(-m_f g - f_{z,b} + f_{z,f})\,\dot{v}_{CG}\,dt = -\int m_f\ddot{v}_g\dot{v}_{CG}\,dt \tag{13}$$

and

$$\int(K_r\phi + C_r\dot{\phi} - f_{z,b}\frac{D}{2}\phi - f_{z,f}\frac{D}{2}\phi + f_{x,b}\frac{D}{2} - K_b\theta^{rel} - C_b\dot{\theta}^{rel} + I_f\ddot{\phi} + \sum_{i=1}^{m} f_{h,i}d_i - \sum_{i=1}^{m} f_{h,i}\phi\frac{W_{sb}}{2} + \sum_{j=1}^{n} f_{s,j}\phi l_j - \sum_{j=1}^{n} f_{s,j}\frac{D}{2})\,\dot{\phi}_{CG}\,dt = 0 \tag{14}$$

Next, we group the energy terms, according to their physical nature, into the following categories:

$E_K(t)$ = kinetic energy

$E_P(t)$ = potential energy of gravity forces

$E_D^{bldg}(t)$ = damping energy dissipated in the building

$E_S^{bldg}(t)$ = recoverable elastic strain energy in the building

$E_D^{soil}(t)$ = energy dissipated by "dashpots" of the soil

$E_S^{soil}(t)$ = elastic strain energy in the soil

$E_Y^{soil}(t)$ = irrecoverable hysteretic energy in the soil

$E_{S+Y}^{soil}(t) = E_S^{soil}(t) + E_Y^{soil}(t)$

$E_I(t)$ = total earthquake input energy.

First, based on Equations (9) through (14), the earthquake input energy is the sum of all the right hand side terms

$$E_I(t) = -\int[m_b\ddot{u}_g\dot{u}_b + m_b\ddot{v}_g\dot{v}_b + (m_b\ddot{u}_g H + m_b\ddot{v}_g H\phi_b)\dot{\phi}_b + m_f\ddot{u}_g\dot{u}_{CG} + m_f\ddot{v}_g\dot{v}_{CG}]\,dt \tag{15}$$

The kinetic energy associated with the absolute motion of the two masses is

$$E_K(t) = \int\{m_b(\ddot{u} + \frac{D}{2}\ddot{\phi} + H\ddot{\phi}_b)\dot{u}_b + [m_b(\ddot{u} + \frac{D}{2}\ddot{\phi})H + I_O\ddot{\phi}_b]\,\dot{\phi}_b + m_f\ddot{u}\dot{u}_{CG} + I_f\ddot{\phi}\,\dot{\phi}_{CG}\}dt \tag{16}$$

It can be seen that $E_K(t)$ is equal to the integrals of the inertial forces with respect to their absolute velocities. The potential energy associated with the gravity forces is

$$E_P(t) = -\int(m_b g\dot{v}_b + m_b g H\phi_b\dot{\phi}_b + m_f g\dot{v}_{CG})\,dt \tag{17}$$

The energy dissipated by viscous damping in the building can be calculated from

$$E_D^{bldg}(t) = \int C_b(\dot{\theta}^{rel})^2\,dt \tag{18}$$

The recoverable strain energy of the building (for linear response) is

$$E_S^{bldg}(t) = \frac{1}{2}K_b(\theta^{rel})^2 \tag{19}$$

For this illustration, the building is assumed to deform in linear manner only, and the irrecoverable hysteretic energy in the building will be zero. Then, the energy dissipated by the dashpots in the soil is

$$E_D^{soil}(t) = \int(\sum_{i=1}^{m} f_{h,i}^D + \sum_{j=1}^{n} f_{s,j}^D)\,\dot{u}\,dt + \int C_r\dot{\phi}^2\,dt + \int\{\sum_{i=1}^{m} f_{h,i}^D(d_i - \frac{W_{sb}}{2}\phi) + \sum_{j=1}^{n} f_{s,j}^D(l_j\,\phi - \frac{D}{2})\}\,\dot{\phi}\,dt \tag{20}$$

The energy dissipated by the yielding and by the recoverable strain energy of the soil can be obtained from

$$E_{S+Y}^{soil}(t) = \int(\sum_{i=1}^{m} f_{h,i}^S + \sum_{j=1}^{n} f_{s,j}^S)\,\dot{u}\,dt + \int K_r\phi\,\dot{\phi}\,dt + \int\{\sum_{i=1}^{m} f_{h,i}^S(d_i - \frac{W_{sb}}{2}\phi) + \sum_{j=1}^{n} f_{s,j}^S(l_j\,\phi - \frac{D}{2})\}\,\dot{\phi}\,dt \tag{21}$$

in which

$$E_S^{soil}(t) = \sum_{i=1}^{m}\frac{(f_{h,i}^S)^2}{2k_{h,i}} + \sum_{j=1}^{n}\frac{(f_{s,j}^S)^2}{2k_{s,j}} + \frac{K_r\phi^2}{2} \tag{22}$$

where $k_{h,i}$ and $k_{s,j}$ are the initial stiffness coefficients of the inelastic soil.

Based on these energy "components," the statement of energy balance of the system is then expressed as

$$E_K(t) + E_P(t) + E_D^{bldg}(t) + E_S^{bldg}(t) + E_D^{soil}(t) + E_{S+Y}^{soil}(t) = E_I(t) \tag{23}$$

The foregoing analysis of the non-linear system models the energy components of the simple non-linear SSI system in Figure 3, rather than that of the fixed-base system (e.g., Akiyama, 1985, 1988, 1997; Anderson and Bertero, 1969; Uang and Bertero, 1988, 1990). Comparing Equation (23) with Equation (1), the simplifications and omissions in Equation (1) become clear.

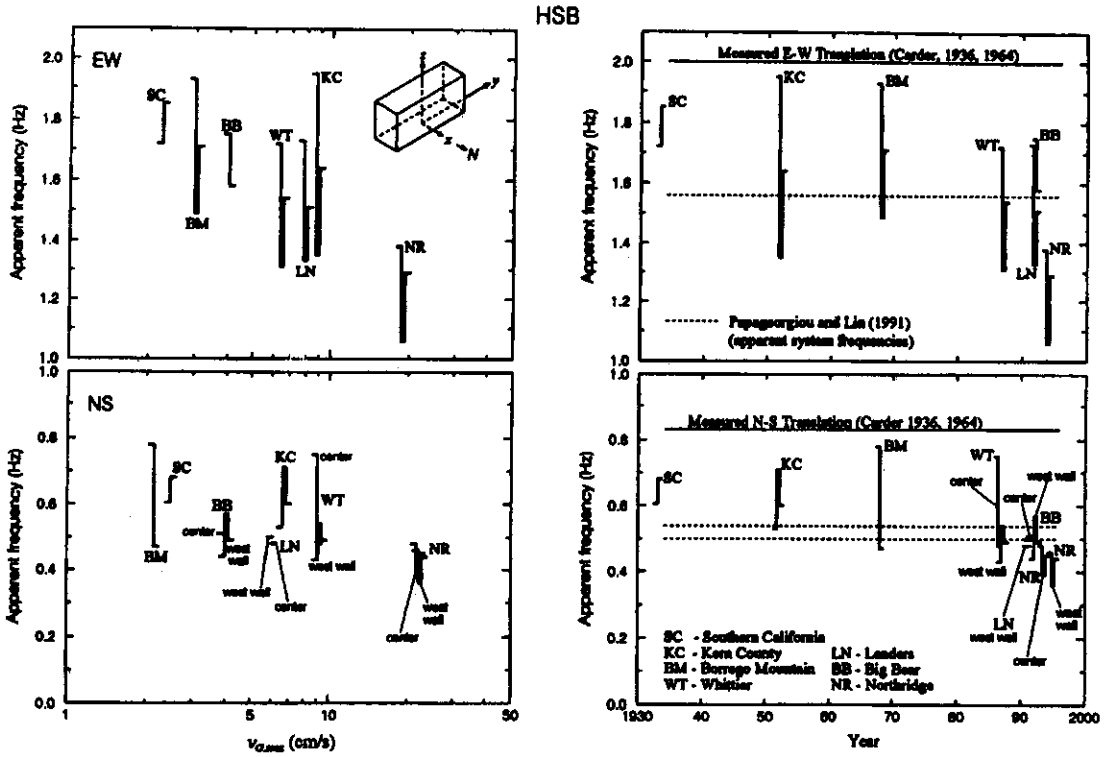

Fig. 6 Schematic diagram of the observed variations of the EW (top) and NS (bottom) system frequencies, f_p, of the Hollywood Storage Building versus peak measured ground velocity, $v_{G,max}$ (left), and time (right), during seven earthquakes (for each earthquake, the horizontal ticks represent pre- and post-earthquake estimates of the system frequencies)

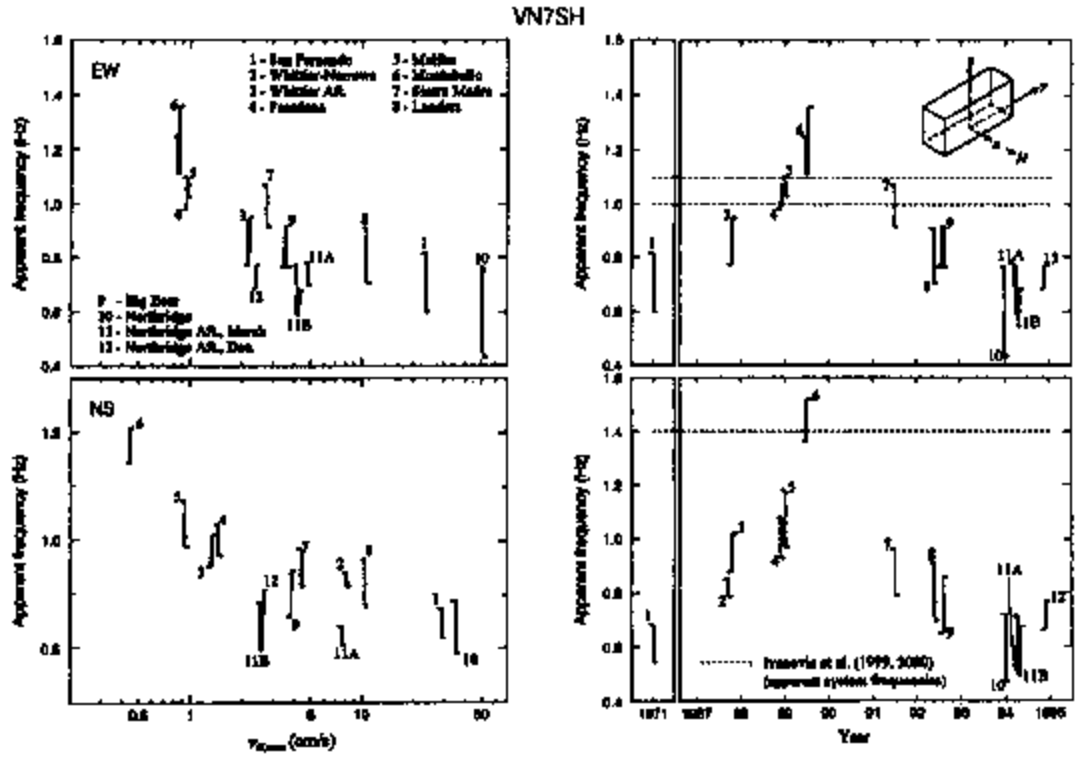

Fig. 7 Same as Figure 6 but for the Van Nuys 7-story hotel

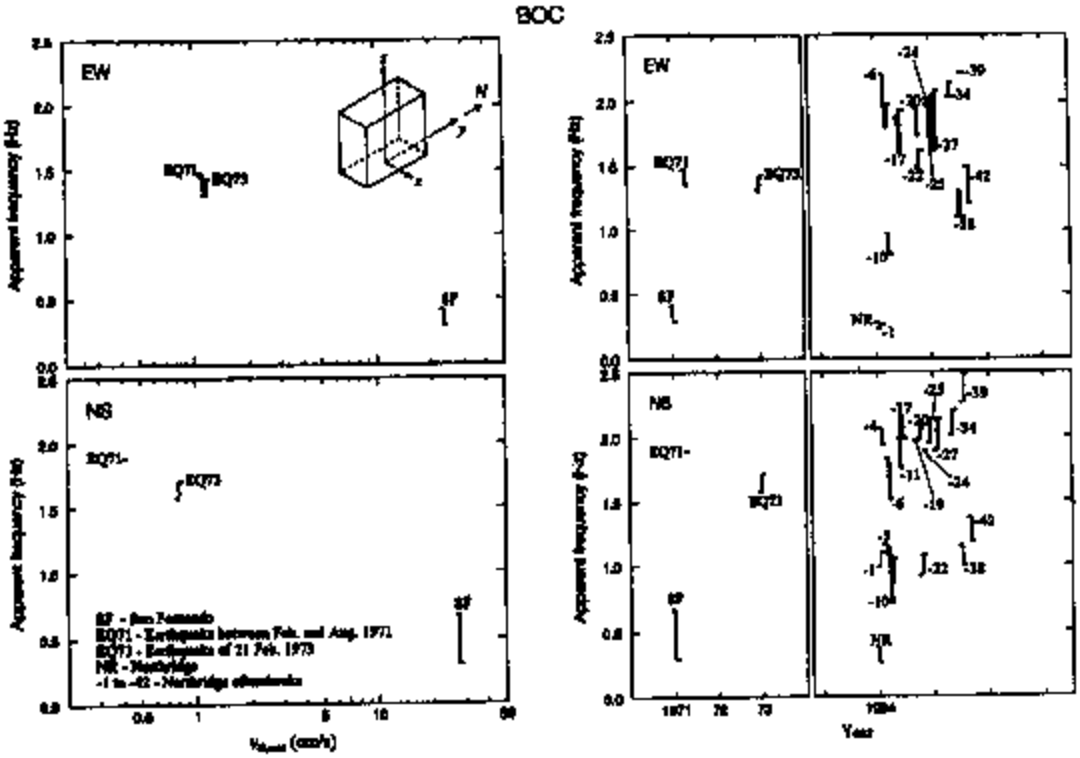

Fig. 8 Same as Figure 6 but for the Bank of California building

EXAMPLE STUDIES OF FIVE BUILDINGS

To illustrate the behavior of the model for energy partitioning in a soil-structure system, shown in Figure 3, Trifunac et al. (2001f) and Hao (2002) analyzed the Hollywood Storage building (HSB), the Van Nuys seven story hotel (VN7SH), the Sherman Oaks Bank of California building (BOC), the Pasadena (Caltech) Millikan Library (MLK), and the Santa Susana ETEC building #462 (ETEC). These five buildings have been studied previously by many investigators (see references in Trifunac et al., 2001f; Trifunac et al., 2001a, 2001b; and Trifunac and Todorovska, 2001). There are multiple recordings in the buildings of weak, intermediate and strong earthquake responses, and three of these buildings were tested using ambient vibration methods. All, except the Santa Susana ETEC building, are reinforced concrete structures and the sites lie on recent alluvium. The ETEC building is a steel structure, and its site lies on sandstone bedrock, which makes the response of this building different from the others.

The building descriptions and the earthquake recordings are described in Hao (2002) and will not be repeated here.

1. Analysis of Recorded Motions: Time and Amplitude-Dependent Response

To evaluate the changes of the system frequency, f_p, during a particular earthquake motion, as a function of the level of response and of the previous response history, the "instantaneous" value of the system predominant frequency, f_p, was approximated by two methods: (1) zero-crossing analysis and (2) moving window Fourier analysis. To isolate the lowest frequency mode, the data was band-pass filtered. The cutoff frequencies for the band-pass filter were chosen to include the system frequency, and were determined after analyzing the instantaneous transfer-functions between the relative horizontal motions recorded on the roof and at the base. The zero-crossing analysis consisted of determining the half periods for all approximately symmetric peaks in the relative response, assuming that the filtered relative displacements can be approximated locally by a sine wave.

Figure 5 shows geographical distribution of the buildings studied here and of the earthquakes which contributed to the recorded data. Figures 6 through 10 show schematically the observed variations of f_p versus $v_{G,\max}$ (the peak measured ground velocity at the base of the building) and time. In these figures, f_p is proportional to the square root of the system stiffness, while $v_{G,\max}$ can be related to the strain levels in the supporting soil. Excluding the EW response of ETEC building, it appears that these soil-building systems behave like non-linear soft spring systems. For $v_{G,\max} \leq 1$ cm/s, the system frequency of the EW response of ETEC building increases with increasing $v_{G,\max}$ ("stiffer" non-linear response). Beyond $v_{G,\max} \approx 1$ cm/s, the system frequency becomes slightly smaller.

The evaluation of the instantaneous system frequency requires complete recordings on the roof and at the base. However, during the 1994 Northridge earthquake and its aftershocks, only the motions on the roof were recorded in the Bank of California building (BOC; Figure 8). The possibility and accuracy of performing the approximate analysis, using motions on the roof only, are discussed in Hao (2002).

Figures 6 through 10 also summarize the time-dependent changes of the instantaneous system frequency, f_p, for the recorded earthquakes ordered in chronological order. Figures 6, 7 and 9 also compare the variations in the system frequencies during strong-motion with the values from low amplitude testing (horizontal lines).

The amplitude-dependent changes of f_p are illustrated in Figures 11 and 12, by plotting f_p versus the corresponding amplitude of the envelope of the analyzed data. Based on the time- and amplitude-frequency analyses, we found that the predominant system frequencies change from one earthquake to another, and also during the response to a particular earthquake. The results also indicate that what is "loosened" by the severe strong motion shaking, appears to be "strengthened" by aftershocks and by intermediate and small earthquakes. The changes of the system frequency of the ETEC building were the smallest (Figure 12). The ETEC building is a steel structure founded on hard bedrock. It experienced no damage during the 1994 Northridge earthquake.

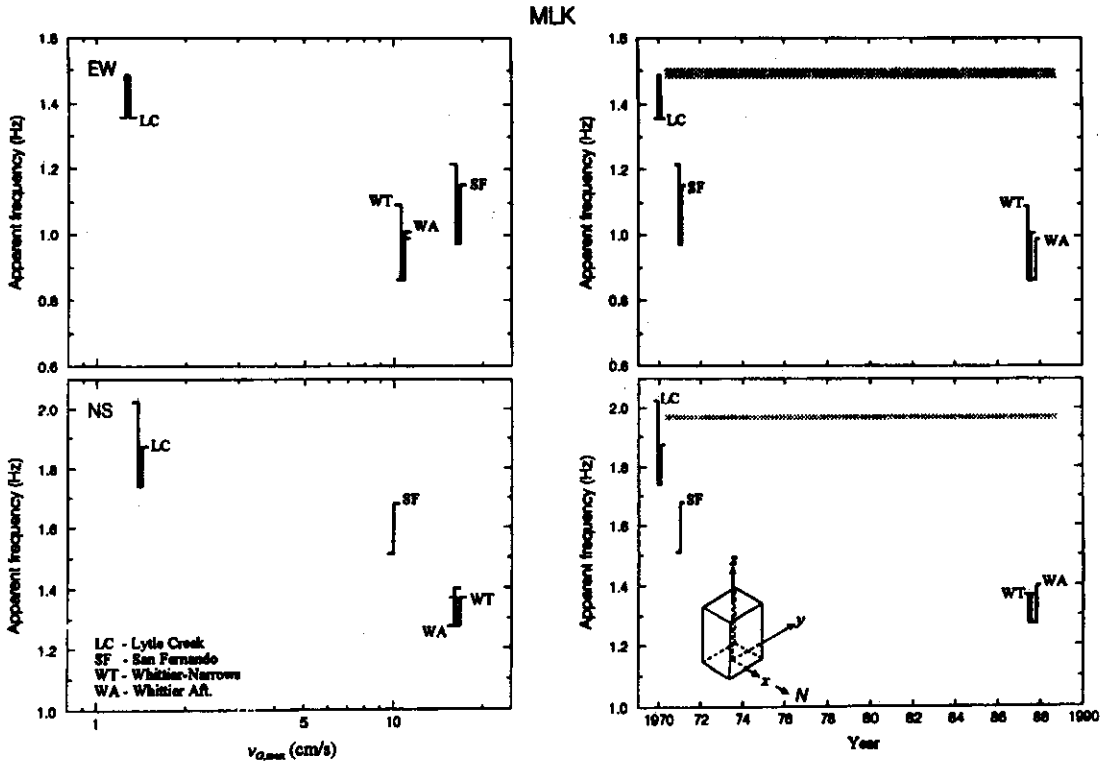

Fig. 9 Same as Figure 6 but for the Millikan Library building

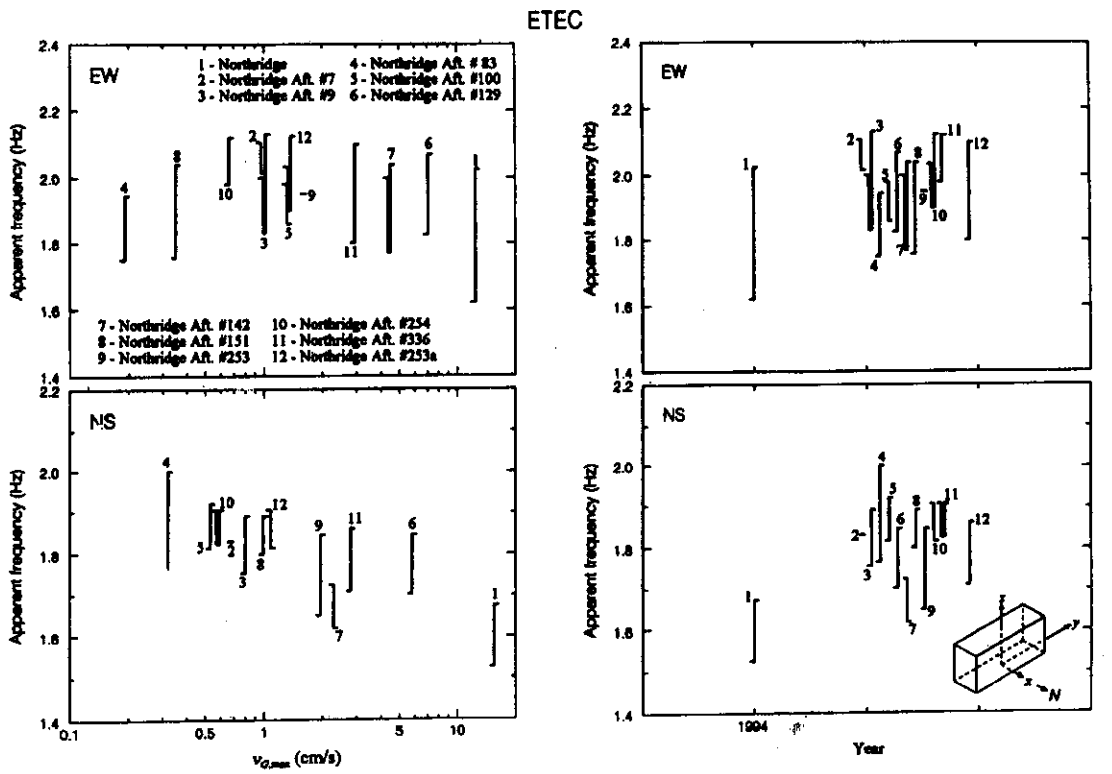

Fig. 10 Same as Figure 6 but for the ETEC building

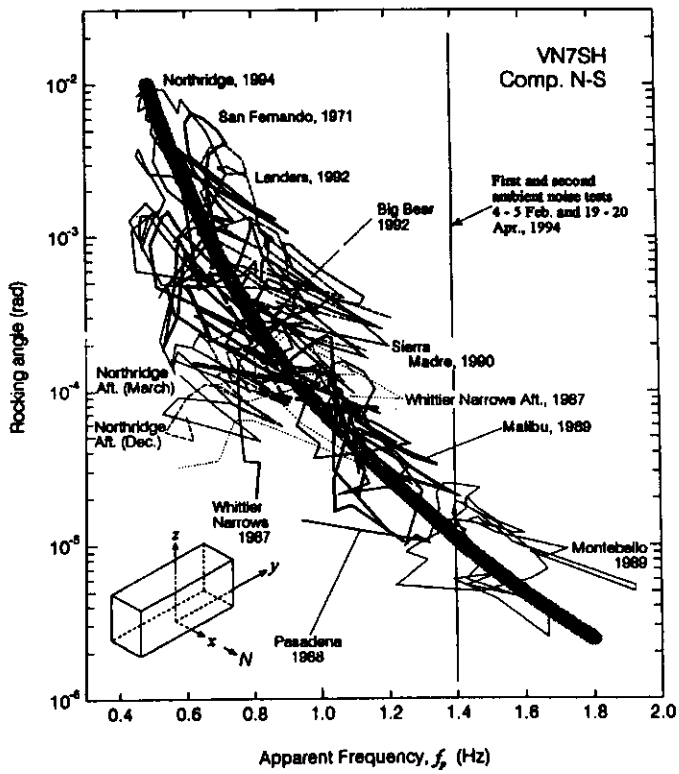

Fig. 11 Dependence of the apparent system frequency of Van Nuys 7-story hotel on the peak amplitude of the NS relative response (rocking angle) (the solid lines show estimates of the system frequencies determined from ambient vibration tests by Ivanović et al., 1999, 2000)

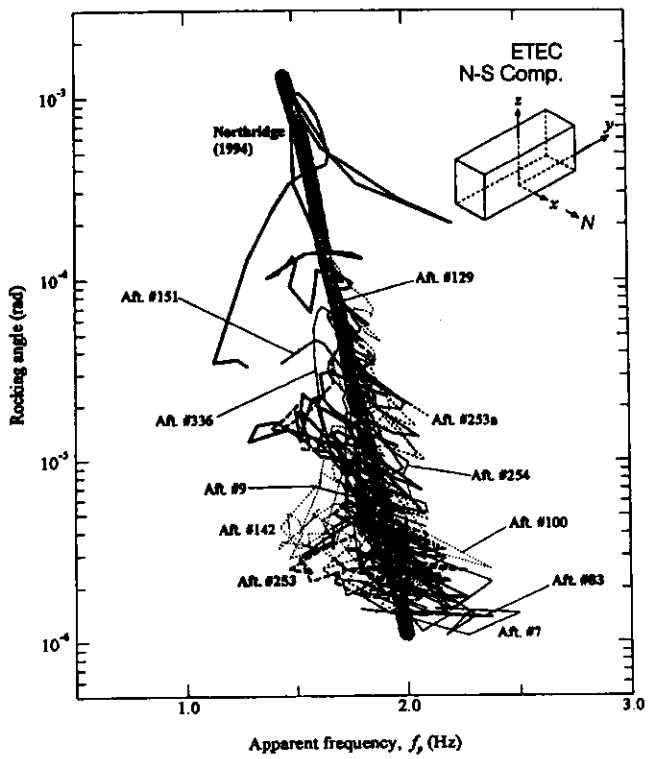

Fig. 12 Dependence of the apparent system frequency of Santa Susana ETEC building on the peak amplitude of the NS relative response

2. Numerical Response Simulation

The accelerations recorded at the base of the buildings were used by Hao (2002) and Trifunac et al. (2001f) as the input excitations for the idealized mathematical model. The values of the model parameters corresponding to the five studied structures are presented and discussed in detail in Hao (2002). From the equations of motion, the unknown displacements were solved numerically in the time domain. Then the associated system energies were determined. In the following, we summarize the results of their simulation, compare the recorded and predicted responses, and discuss the system energies.

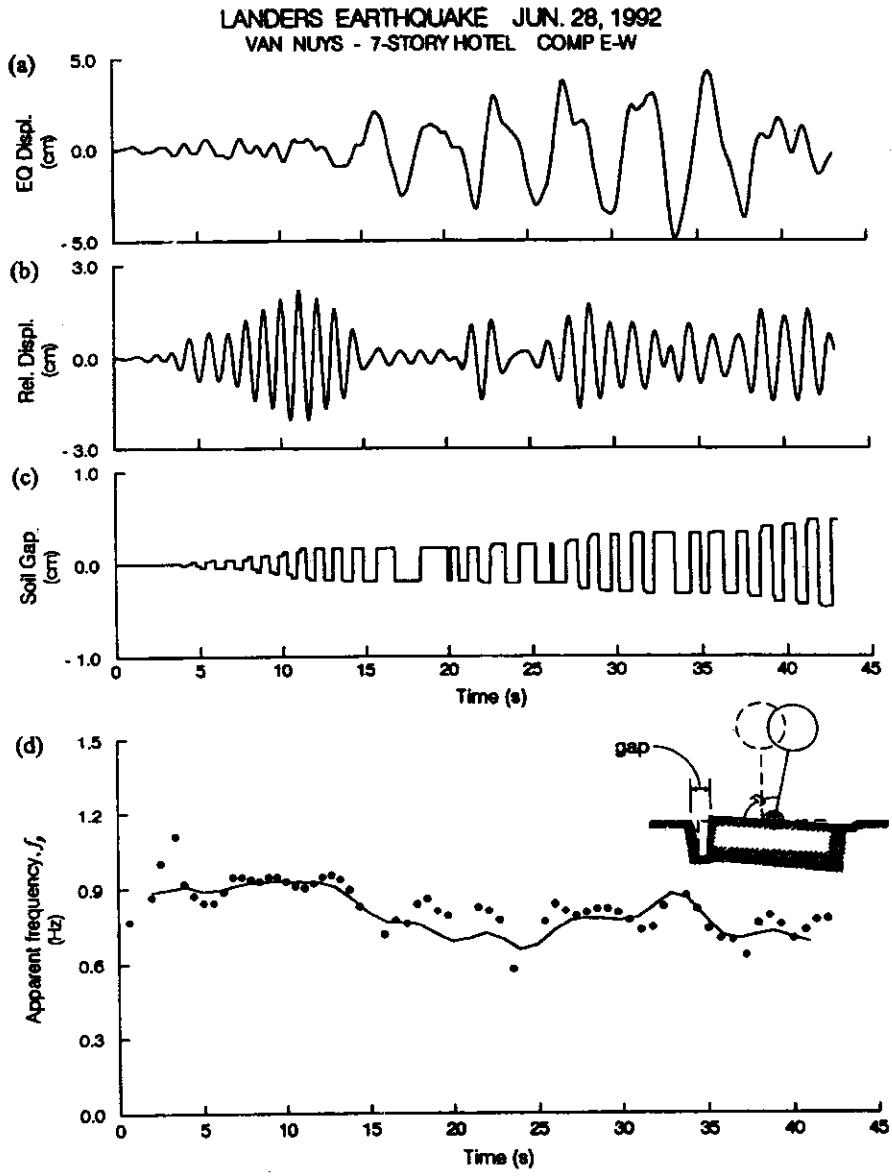

Fig. 13 An example of predicted response for the 1992 Landers earthquake modeling the EW response of VN7SH building

2.1 Predicted Responses

Figure 13 illustrates sample results of the simulated response of the VN7SH building EW response for 1992 Landers earthquake. Part (a) of Figure 13 shows the displacement recorded at the base of the building, which is used as input excitation for the simulation. The predicted displacement of the roof relative to the base is plotted in part (b). During the shaking, the soil on the sides of the foundation is

pushed sideways by the vibration of the foundation. This is shown in part (c) (the gaps shown here represent the separations at the surface level). Part (d) of this figure shows the results of the zero-crossing (solid points) and of the moving window Fourier (solid lines) analyses for the changes of system frequency. In part (c) of Figure 13, it is found that the separation between the foundation and the side-soil occurs at 3.9 s and keeps increasing between 3.9 to 6.0 s. The system is oscillating with partially contacting the soil springs on the sides, and the system stiffness decreases a little. At about 7.35 s, the larger vibration of the foundation pushes the soil on the sides further. This phenomenon increases the system stiffness (i.e. increases f_p). Again, the gap increases between 7.35 to 12.0 s and when the system is oscillating without touching the soil on the sides (between 12 to 22 s), the system stiffness decreases. This phenomenon, referred to as "pinching," can also be seen at about 27.0, 30.9 and 37.7 s.

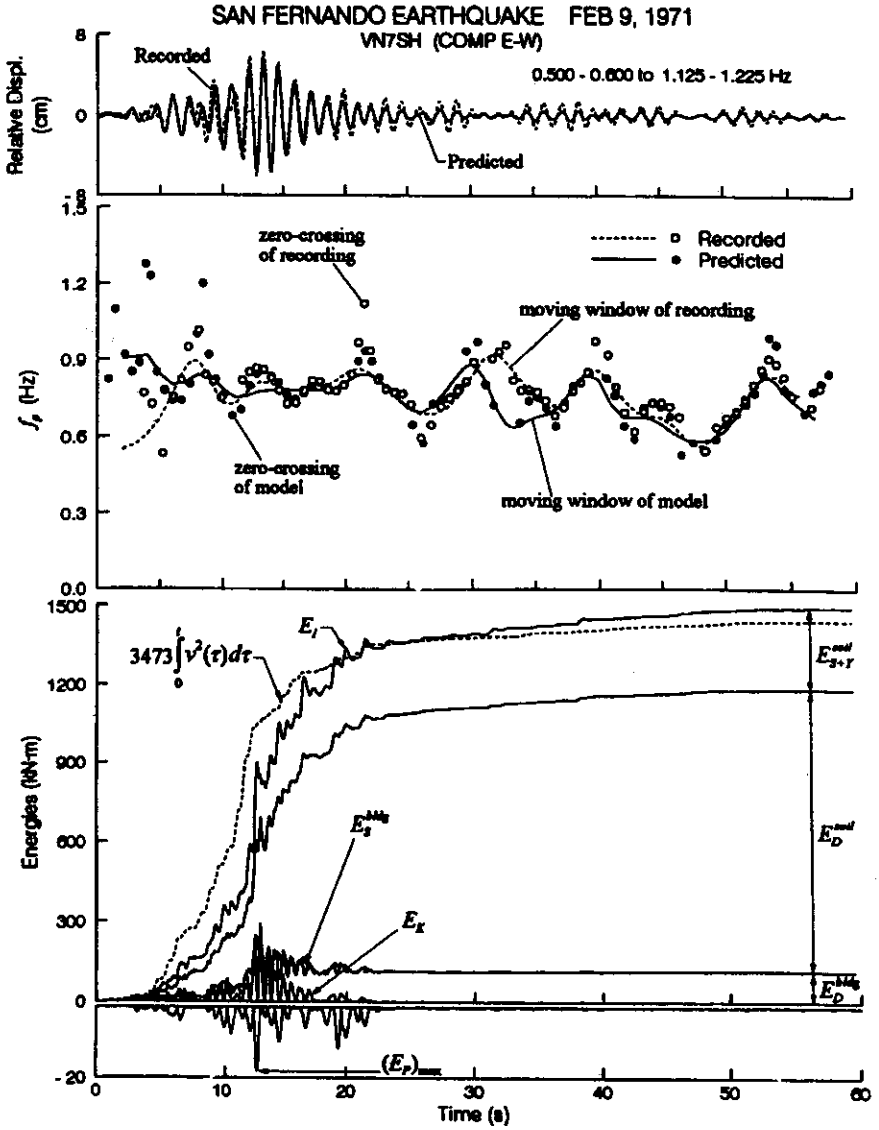

Fig. 14 Top: comparison of recorded (dashed line) and predicted (solid line) EW relative displacement response at the roof of VN7SH during the 1971 San Fernando earthquake; center: time dependent changes of the system frequency f_p computed from recorded (dashed line and open circles) and predicted (continuous line and solid dots) responses; bottom: contributions to the system energy: E_{S+Y}^{soil}, E_D^{soil}, E_S^{bldg}, E_D^{bldg}, E_K and E_P and their sum E_I (input wave energy $a_0\int_0^t v^2(\tau)\,d\tau$ is shown by dashed line)

2.2 Comparison of the Recorded and Predicted Responses

Figure 14 shows an example of the predicted response together with the recorded response of the VN7SH during 1971 San Fernando earthquake. The top part of Figure 14 shows a comparison of the band-pass filtered relative response of recorded motions (dashed line), and the simulated motions (solid line) using the model presented in Figure 3. The central part of Figure 14 shows the time-dependent changes of the system frequency, f_p. The dashed lines show the changes in f_p evaluated by moving window Fourier analysis of the recorded data, and the open circles show the estimates by the zero-crossing analysis also using the recorded data. The solid line and solid points show the corresponding quantities for the predicted response. A complete set of figures showing further details of these results for HSB and VN7SH buildings during all recorded earthquakes can be found in Trifunac et al. (2001f). The results corresponding respectively to the BOC, MLK and ETEC buildings are presented in Hao (2002).

The bottom part of Figure 14 shows a comparison of the predicted total system energy with the input wave energy (detailed discussion on the "input wave energy" can be found in Trifunac et al., 2001f). The distribution of the predicted total system energy, E_I, among E_D^{bldg}, E_S^{bldg}, E_D^{soil}, E_{S+Y}^{soil}, E_k and $(E_P)_{max}$ is also illustrated in this figure.

2.3 Energies of the System

The bottom part of Figure 14 shows a comparison of the predicted total system energy with the input wave energy versus time. To properly compare these results, we band-pass filtered the model results and the input wave energy (the processed velocity was filtered before integration). In these figures, the top solid line represents the sum of different partitions of energy resulting in the "total" system energy, E_I. The dotted line represents $a_0 \int_0 v^2(\tau)\, d\tau$, with a_0 determined by least squares fit of the "total" energy in terms of $\int_0 v^2(\tau)\, d\tau$. As explained in Trifunac et al. (2001f), the integral $a_0 \int_0 v^2(\tau)\, d\tau$ represents the cumulative energy arriving at the site in the form of seismic waves. The "total" energy represents the sum of all response energies of the soil-structure system (Figure 3).

In fitting the data for the total system energy in terms of the input wave energy for different earthquake excitations, it can be assumed that the relationship is linear; that is

$$y = a_0 x \tag{24}$$

or

$$y = a_1 x + b_1 \tag{25}$$

where x and y represent $\int_0 v^2(\tau)\, d\tau$ and E_I, respectively; and a_0, a_1 and b_1 are constants.

Figures 15 through 19 show the trends of the computed E_I (total energy of the soil-structure system response) versus $\int_0 v^2(\tau)\, d\tau$ (input wave energy factor) for the EW (solid circles) and NS (solid triangles) responses of five selected buildings, for all recorded earthquakes. For the 1970 Lytle Creek and 1971 San Fernando earthquakes recorded in the HSB, the system energies are predicted based on assumed model parameters only, since without recorded roof motion, it is not possible to find the best estimates of the system parameters. The least squares fit through the data gives $\bar{a}_0 = 1.71\times10^4$ kg/s for the HSB, $\bar{a}_0 = 0.48\times10^4$ kg/s for the VH7SH, $\bar{a}_0 = 1.55\times10^4$ kg/s for the BOC, $\bar{a}_0 = 4.11\times10^4$ kg/s for the MLK, and $\bar{a}_0 = 0.56\times10^4$ kg/s for the ETEC building. In Figure 17, the earthquake motions at the ground floor in the Bank of California building were recorded only during the 1971 San Fernando earthquake and its aftershocks, between 9 February and 4 August 1971, and during the earthquake of 21 February 1973. Because there are not enough data, $\bar{a}_1$ and $\bar{b}_1$ are not considered in this case.

For vertically incident plane shear waves, and neglecting the wave scattering from the foundation, the coefficient a_0 should be approximately equal to $\rho_s A\beta$, where ρ_s is density, β is the shear wave velocity in the soil surrounding the foundation, and A is the area of the plan of the building foundation (Trifunac, 1995; Trifunac and Brady, 1975; Trifunac et al., 2001f). Tables in Hao (2002) present values

for ρ_s, β, plan dimensions and computed $\rho_s A\beta$ for each building. From those tables, we obtain $a_0' = \rho_s A\beta/10^4 = 3.6\times10^4$ kg/s for HSB, $a_0' = 3.0\times10^4$ kg/s for VN7SH, $a_0' = 3.2\times10^4$ kg/s for BOC, $a_0' = 4.6\times10^4$ kg/s for MLK and $a_0' = 3.5\times10^4$ kg/s for ETEC building. It is seen that $a_0' \log_{10} \int_0 v^2(\tau)\, d\tau$ is an upper bound for all points shown in Figures 15, 16 and 19. With increasing amplitudes of shaking, the effective $\rho_s A\beta$ reduces. The effective $\rho_s A\beta$ is reduced, because the strong ground motion does not consist of plane vertically arriving S-waves, and is a complex sequence of body and surface waves whose angles of approach vary vertically and horizontally. Furthermore, coefficients a_0 and a_1 depend on the soil-structure interaction, which involves various types of foundation systems. We conclude that considering the complexities of the energy transfer from the soil into the building (Trifunac et al., 1999a; 2001b; 2001f), the agreement of the predicted E_I versus $\int_0 v^2(\tau)\, d\tau$ is satisfactory to warrant further and more detailed studies of the energy transfer mechanisms. Therefore, if the input wave energy factor, $\int_0 v^2(\tau)\, d\tau$, of the strong motion at a given site is known, it is possible to estimate approximately the total system energy, E_I, for an expected future earthquake.

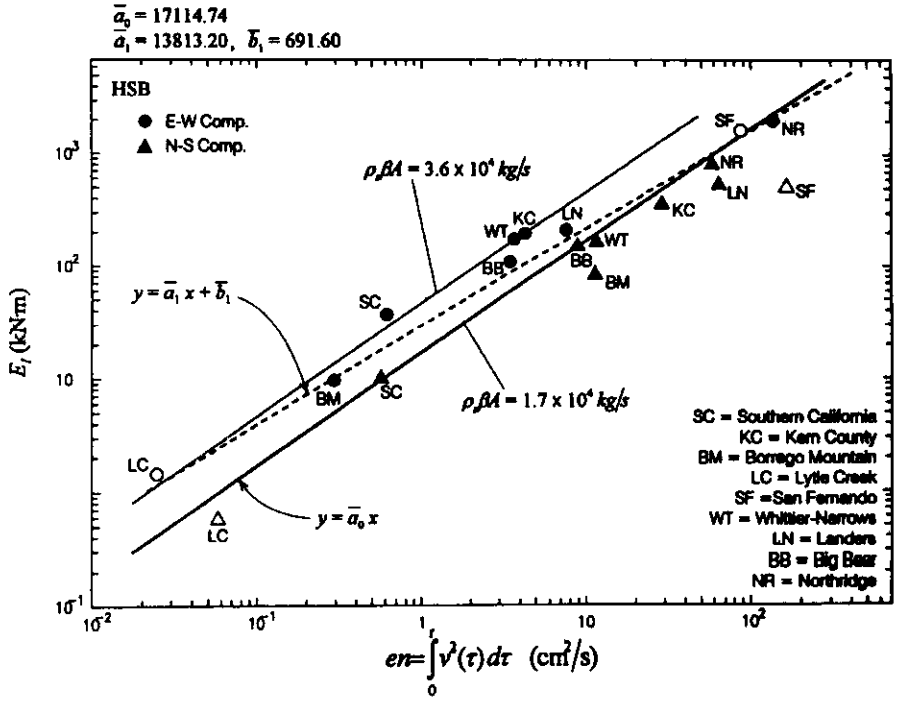

Fig. 15 Total computed response energy E_I (kN·m) versus input energy factor, *en*, for nine earthquakes recorded in the HSB

ENERGY-BASED DESIGN CONSIDERATIONS

For design purposes, it is important to define the meaning of "energy demand". Uang and Bertero (1990) defined the input energies E_i *and* E_i' (absolute and relative) in terms of the relative response of a fixed-base SDOF model subjected to horizontal ground motion only. They used these energies to convert the results to an equivalent spectral velocity and proposed the input energy equivalent velocity spectra for future design. It should be noted that the equivalent spectral velocity depends on the vibration period of the buildings and the predominant periods of the earthquake ground motions. Furthermore, the soil-structure interaction effects were not considered by Uang and Bertero (1990). Consequently, their approach is not fundamentally different from the classical Response Spectrum Method. In the following, we use the model in Figure 3 and the energy of incident ground motion, to develop more realistic

procedures for estimation of the energy demand. Then the designer has to decide how to balance this demand with all available resources, including the energy absorption capacity of the supporting soils.

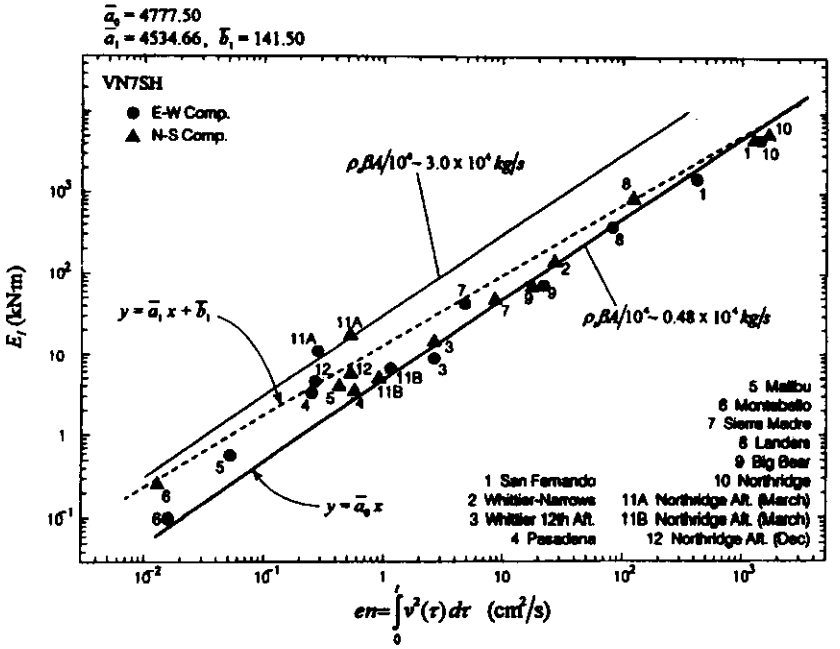

Fig. 16 Total computed response energy E_I (kN·m) versus input energy factor, *en*, for twelve earthquakes recorded in the VN7SH

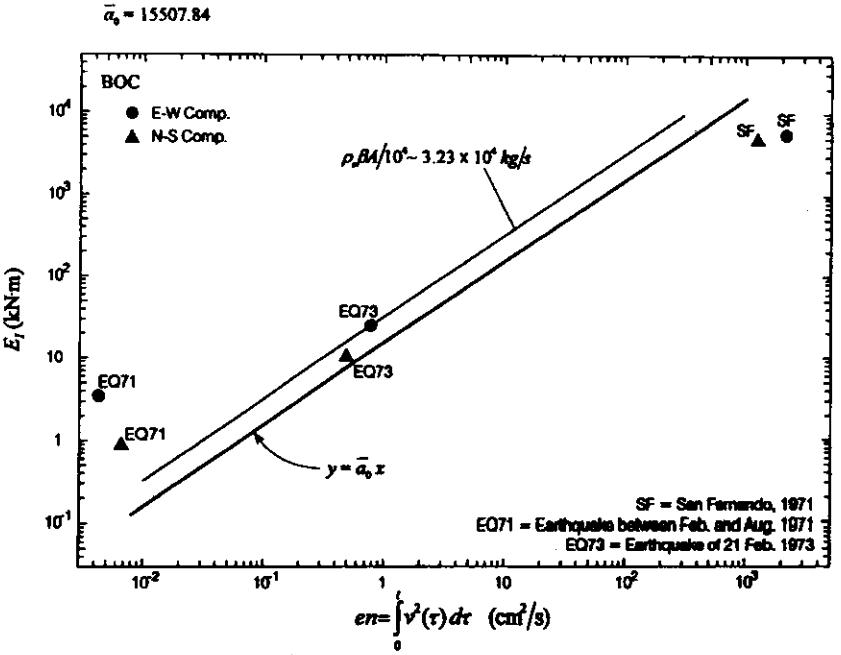

Fig. 17 Total computed response energy E_I (kN·m) versus input energy factor, *en*, for three earthquakes recorded in the BOC

1. Energy Demand

For a building supported by flexible soil, the soil-structure interaction will lead to horizontal and rocking deformations of the soil, and in general, this will reduce the amplitude of the strong-motion

pulses entering the structure. Partitioning of the incident seismic wave energy into horizontal and rocking motions of the soil-foundation-building system and scattering of the incident waves from the foundation will thus reduce the energy available to cause relative deformation of the structure. This implies that the effective energy to be absorbed by structural damping and hysteretic response of structures (for non-linear response) will be less than the traditional estimates, which consider the system as a fixed-base model (the case of "rigid" soil without soil-structure interaction).

Figures 20a and 20b illustrate the maximum kinetic energy, $(E_K + E_P)_{max}$ versus $E_I^* + E_I$ for VN7SH structure, where E_I^* = the total system response energy computed at the instant when $(E_K + E_P)_{max}$ occurs, and E_I = the total system response energy at the end of excitation. This implies that the amplitudes of velocity pulses entering the structure and causing the relative response have been reduced by soil-structure interaction, soil damping, and the energy absorbed by hysteretic response of the soil.

In the use of energy concepts for seismic-resistant design, E_I in Equation (23) represents the demand, and the summation of the left hand side terms shows what should be supplied. It is important to note that this demand does not only deform the building, but also affects the soil-foundation interaction effects. The advantages of not ignoring SSI are apparent. The challenge for future research is to quantify all these energies and to show how those can be estimated for use in design.

2. Energy Absorption Capacity of the Structure – A Case Study (VN7SH)

In the study of Trifunac et al. (2001f), a shear beam model of a building with bilinear force-deformation relation was used to examine some elementary aspects of transient waves propagating in a structure. The results are based on dimensional analysis of the problem and represent conceptual relationships between the amplitude of peak velocity of the wave propagating upwards in the structure, and the energy and power of the response. An application to the VN7SH building is illustrated in the following.

For the EW response of VN7SH building, the maximum accumulated energy, equal to 387 to 442 kN·m is estimated assuming that the building is responding in the linear range of response. The largest power of the incident waves which the VN7SH building can take without damage is estimated to be 1932 to 2208 kN·m/s (Appendix A; Trifunac et al., 2001f). A larger and longer lasting incident wave would force the building to deform monotonically, entering far into the non-linear response amplitude range. The work dissipated by the hysteresis during one quarter of the vibration cycle up to ductility of 2, is estimated to be 1240 to 1414 kN·m, and the associated power in the range from 4816 to 5492 kN·m/s. The work dissipated by the closed hysteretic loop (for one complete cycle of response) is estimated to be between 2480 to 2829 kN·m, and the corresponding maximum power is 2407 to 2746 kN·m/s.

Table 1 Description of the Different Cases Used for Comparison of Relative Response of the Building, Defined Based on whether a Fixed-Base or a Flexible-Base System is Assumed, and whether the Building and Soil are Linear or Non-linear

	Classification					
Case	**Case I**	**Case II**	**Case III**	**Case IV**	**Case V**	**Case VI**
Soil-structure interaction	no	no	yes	yes	yes	yes
Building property	linear	non-linear	linear	non-linear	linear	non-linear
Soil property	–	–	linear	linear	non-linear	non-linear

The above estimates of the building capacity to absorb energy and power are shown by the gray bands in Figure 21a. The three examples, in order of increasing amplitudes, are for (1) monotonic load increasing up to ductility of one (this represents maximum elastic strain energy), (2) one complete cycle of non-linear response (assuming ductility of two), and (3) for monotonic response, during one quarter of the system period, up to the ductility of two. All other transient capacities (e.g., for more than one complete cycle) are larger and therefore not shown in Figure 21a.

The VN7SH building was damaged by the Northridge earthquake of 17 January 1994 and its aftershocks. Clearly, inelastic action took place in the building response. To illustrate the contribution of the non-linearity in the building to the dissipation of energy, we present a comparison of the relative responses assuming fixed-base ("w/o SSI") and flexible-base ("w/ SSI") cases, when the building and soil are linear, and non-linear using the model in Figure 3. The considered cases are summarized in Table 1.

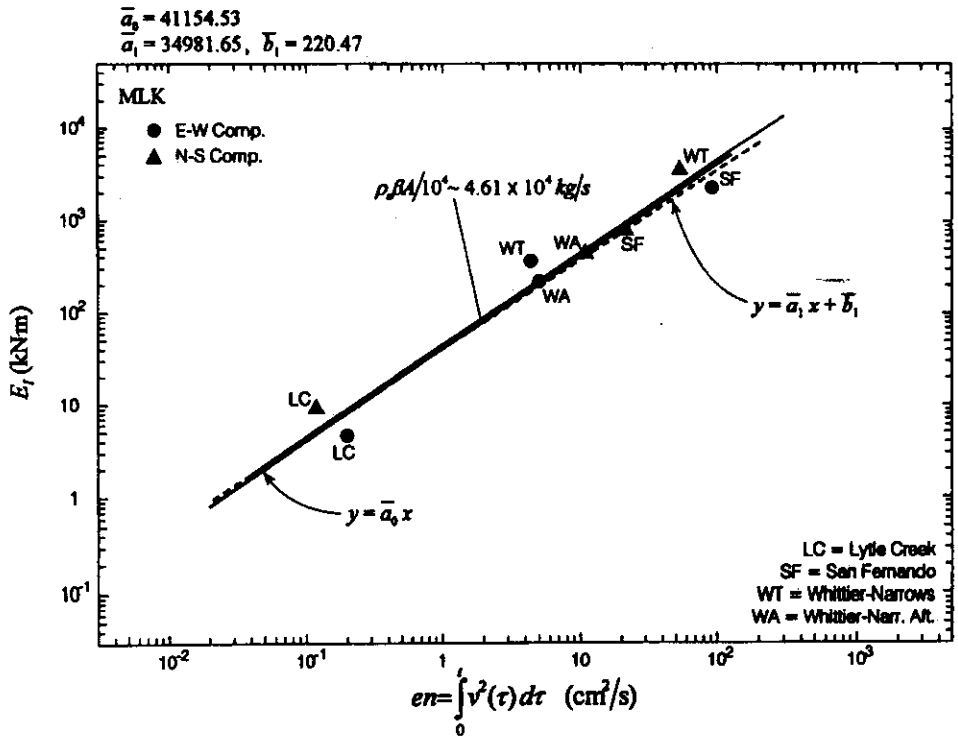

Fig. 18 Total computed response energy E_I (kN·m) versus input energy factor, *en*, for four earthquakes recorded in the MLK

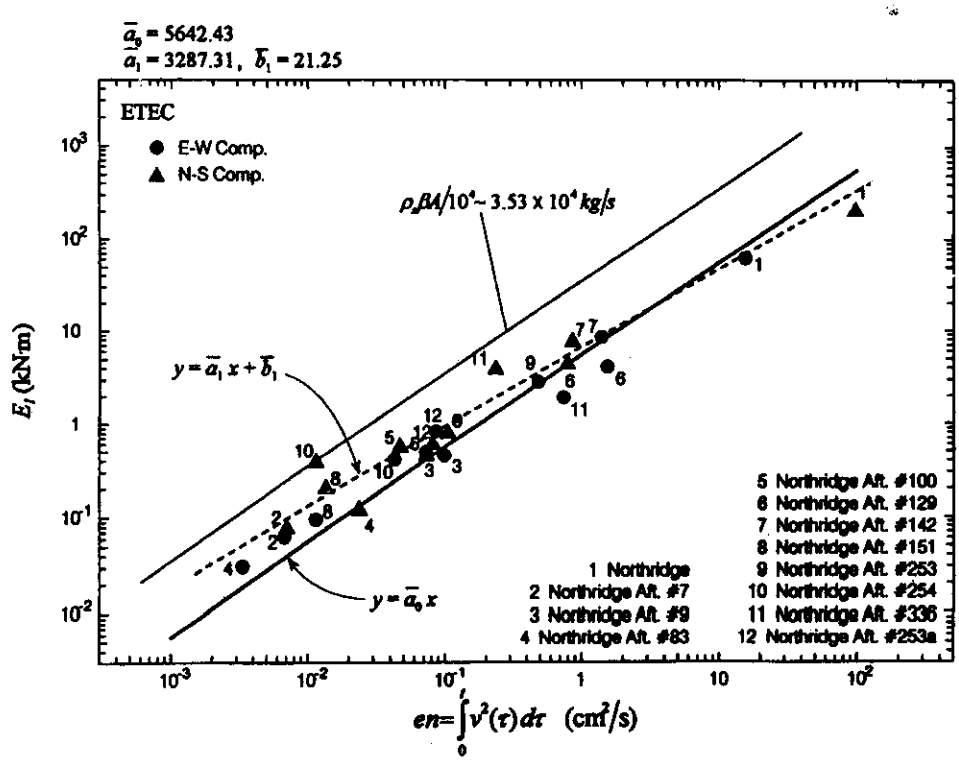

Fig. 19 Total computed response energy E_I (kN·m) versus input energy factor, *en*, for twelve earthquakes recorded in the ETEC

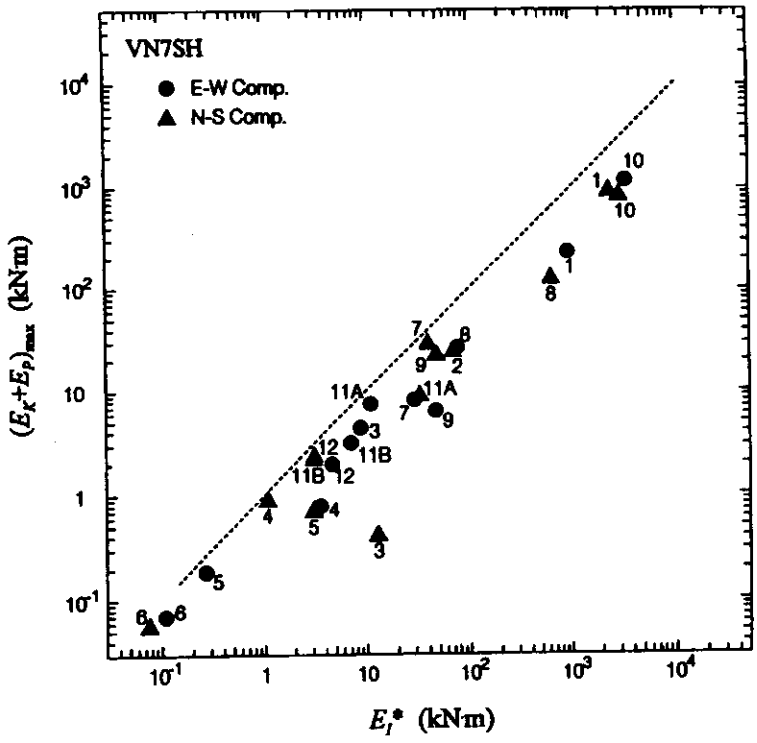

Fig. 20a Total computed kinetic energy $(E_K + E_P)_{max}$ versus E_I^* (kN·m), total system response energy computed at the instant when $(E_K + E_P)_{max}$ occurs, for twelve earthquakes recorded in the VN7SH

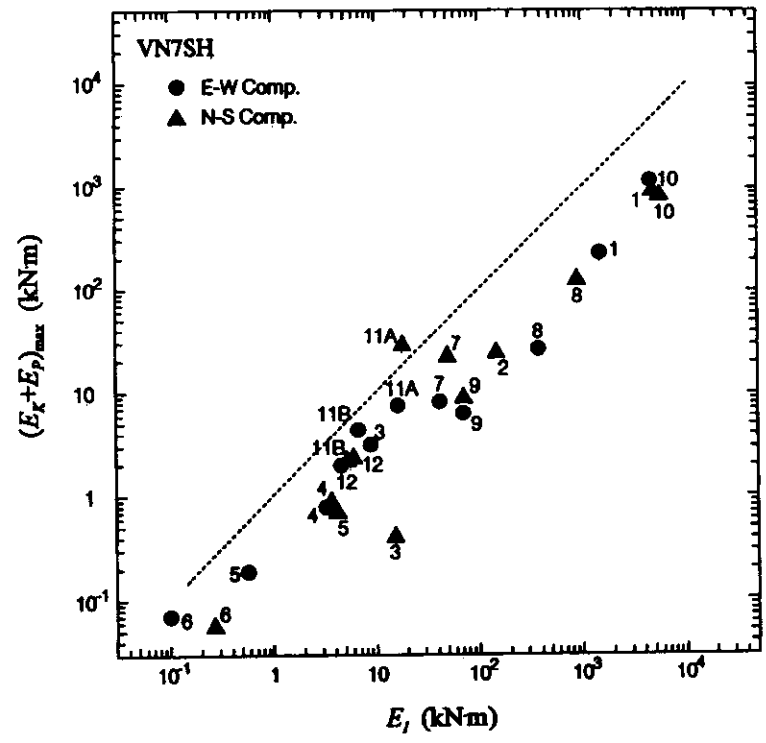

Fig. 20b Total computed kinetic energy $(E_K + E_P)_{max}$ versus E_I (kN·m), total system response energy at the end of excitation, for twelve earthquakes recorded in the VN7SH

The responses plotted in Figures 21a and b were calculated by using the same starting parameters. The 1994 Northridge earthquake was used as input excitation to compare the predictions with the estimated energy and power demands as summarized above (Trifunac et al., 2001f). Figure 21b shows the relative responses of the model in Figure 3. Part (i) of Figure 21b shows the ground velocity during 1994 Northridge earthquake. The relative responses for Cases I and II are plotted in the Part (ii), Cases III and IV are plotted in the Part (iii); and Cases V and VI are plotted in the Part (iv). The dashed lines show the relative responses for linear building, and solid lines show the corresponding quantities for non-linear building.

Top part of Figure 21a shows the sum of all energies in the relative building response (kinetic, potential and hysteretic, when the building models are linear and non-linear), for all of the above cases. It is seen that for the "w/o SSI" cases (Cases I and II), a large ground motion pulse starting at about 3.4 s (see Part (i) of Figure 21b) would have resulted in energy jump of about 590 kN·m, during about 0.22 s, resulting in input power approaching 3000 kN·m/s (see bottom of Figure 21a). This pulse would have deformed the building beyond its linear response range, between 3.5 to 4 s into the earthquake (see also Islam, 1996). In the presence of soil-structure interaction, assuming the soil is linear (Cases III and IV), the amplitude of the incident wave is slightly reduced, and the response energy in the building is reduced by a factor of about 1.25. When the soil is non-linear (Cases V and VI), the amplitude of the incident wave is reduced considerably, and the building continues to respond in essentially a linear manner until 8.4 s into the earthquake. At about 8.9 s and 9.7 s, the SSI model with non-linear soil (Case VI) experiences a sudden jump in the energy of the relative response during short "stiff" episodes of response, for example, during closure of the gaps between the foundation and the non-linear springs representing the soil. Nevertheless, the benefits of not ignoring SSI should be apparent from Figure 21a (top), which shows that the response energy in the building is reduced by a factor of about 3 due to SSI and non-linear soil response. These results lead to the conclusion that if the VN7SH system behaved like a "fixed-base model", the building would have collapsed during the 1994 Northridge earthquake.

3. Duration of Strong Ground Motion

One of the major shortcomings of the classical Biot's response spectrum method (Biot, 1932; 1933; 1934; 1941; 1942) has been its dependence on the peak response amplitude alone, without explicit consideration of the duration of strong shaking and of the rate of arrival of the incident strong motion energy. We use the following example to show why it is important for a realistic design method to reflect the effects of strong motion duration.

Figure 22 shows the time history of two "earthquakes" that result in the same amount of the input wave energy, $\int_0^t v^2\,dt$, but different durations. The energy absorbing capacity of a hypothetical structure is shown by a wide gray line. The integral of Earthquake 1 increases rapidly and tends asymptotically towards its final value, while the integral of Earthquake 2 increases "slowly". The large average and instantaneous power produced by Earthquake 1 will cause damage and collapse of the structure, with design capacity as shown in the figure. Thus it is important to relate the maximum and average power of incident wave energy with the capacity of the structure to absorb this energy, and to choose sufficiently high energy absorbing capacity for safe earthquake-resistant design. Appendix A shows an elementary example of how to estimate the energy absorbing capacity of a hypothetical structure; but these ideas must be developed further, and calibrated against the observed full-scale responses of many structures to damaging levels of strong earthquake ground motion, before this tool can be used in engineering design.

SUMMARY AND CONCLUSIONS

In this work, an alternative (proposed by Trifunac et al., 2001f and Hao, 2002) to the spectral method in earthquake-resistant design is reviewed, by analyzing the flow of energy associated with strong motion, and by focusing on the energy during soil-foundation-structure system response. Starting with the derivation of energy equations, we reviewed the work of Trifunac et al. (2001f) and Hao (2002) on how to identify and how to quantify the energy dissipation mechanisms. For design considerations, it is necessary first to understand and to quantify all these energies, and then to show how it is possible to incorporate maximum power demands into the design process.

To illustrate the energy flow and dissipation through a soil-structure system, as a basic vehicle, a simple model in which both the soil and structural response can be non-linear has been adopted. This

model, shown in Figure 3, consists of a rigid foundation supported by non-linear soil springs, and a structure represented by a single-degree-of-freedom oscillator. For illustration, we summarized the results of Hao (2002) for a 14-story storage building in Hollywood, a 7-story hotel in Van Nuys, a 12-story commercial building in Sherman Oaks, a 9-story library building in Pasadena, and a 8-story research building in Santa Susana, for which processed strong motion data was available. All of the currently processed strong motion data were analyzed, and the simple model was used to quantify approximately the distribution of the incident wave energy. Hao (2002) and Trifunac et al. (2001f) were able to show that there is good correspondence between the estimates of the incident wave energy and the sum of all response energies in the soil-structure system. This result points to the need to research the transfer of the incident wave energy into soil-structure systems.

The above presented results show that a typical soil-structure system is capable of reflecting large fractions of the incident strong motion energy back into the soil by means of scattering (not present for the model in Figure 3) and non-linear soil response. Clearly, the nature of these powerful energy dissipation mechanisms must be carefully studied to provide reliable and verifiable estimates for use in the future earthquake-resistant design. Towards this end, we first reviewed a definition for the energy demand. Hao (2002) and Trifunac et al. (2001f) showed that this demand does not only result in deformation of the building, but also leads to strong soil-foundation interaction effects. Then, we illustrated some elementary aspects of energy absorption capacity of structures, and pointed out the roles of the duration of strong shaking and of the rate of arrival of the incident strong motion energy. The reviewed analyses are, of course, preliminary, but those indicate that there exist major advantages and rational reasons for adoption of power-based description of seismic demands in the design of earthquake-resistant structures.

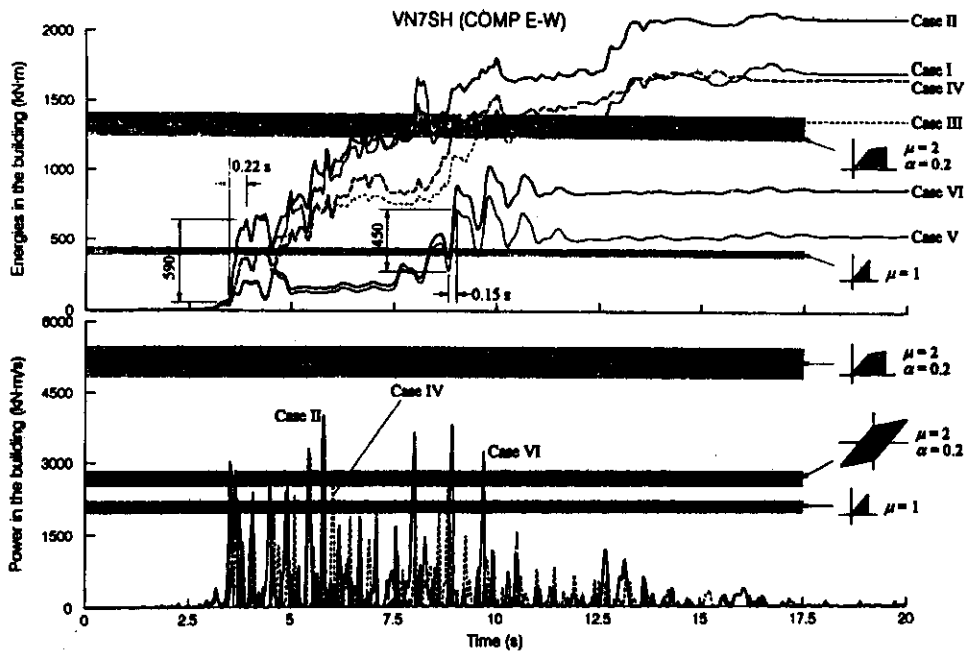

Fig. 21a Comparison of the EW response of VN7SH, during 1994 Northridge earthquake, in the presence and absence of soil-structure interaction, with linear and non-linear soil considerations; top: energies of relative response; bottom: power of relative response

ACKNOWLEDGEMENTS

The material presented in this paper is drawn mostly from the Ph.D. thesis of the author presented to the Graduate School of the University of Southern California in May of 2002. This paper is dedicated to the author's thesis advisor, Professor Mihailo D. Trifunac, on the occasion of his 60th birthday, and in recognition of his leadership and many original contributions to the fields of earthquake engineering and engineering seismology, including work on the topic reviewed in this paper. The author would like to express her most sincere gratitude to Professors M. D. Trifunac and M. I. Todorovska for their guidance throughout her doctoral studies, and for their encouragements and advice.

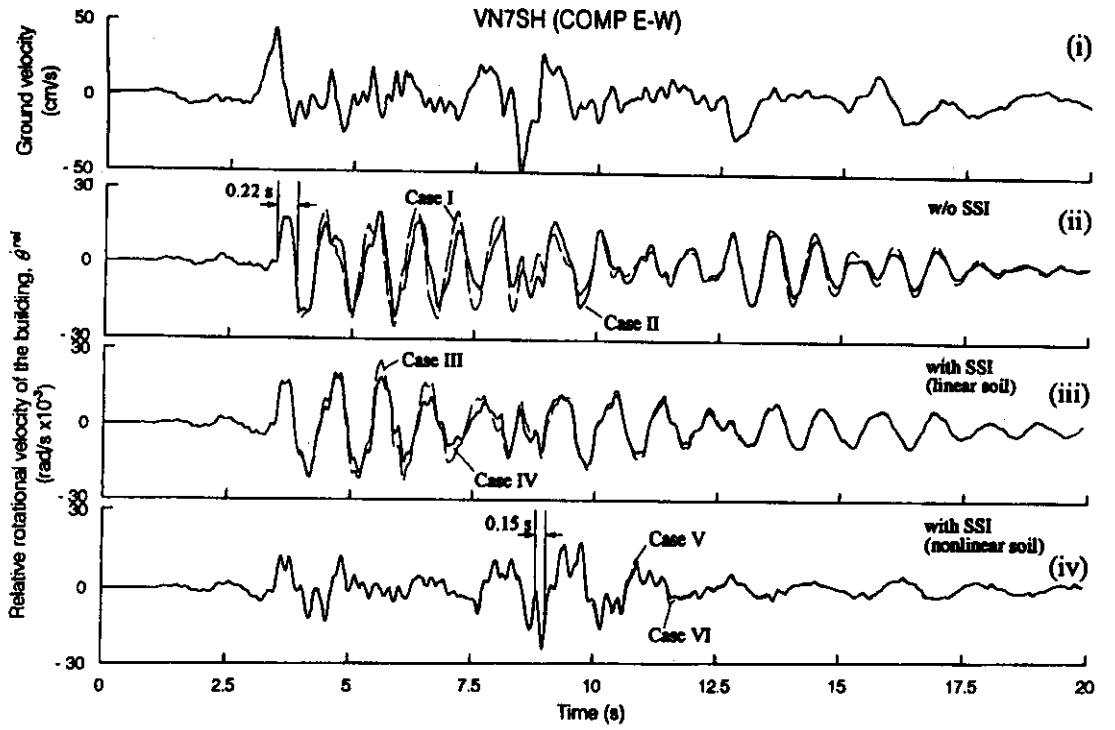

Fig. 21b Comparison of the simulated EW relative velocity response of VN7SH, during 1994 Northridge earthquake, in the presence and absence of soil-structure interaction (dashed lines show the responses for linear building assumption, and solid lines show the corresponding quantities but for non-linear building assumption): (i) ground input velocity, (ii) simulation without soil-structure interaction (SSI) (iii) simulation with SSI assuming soil behaves linearly (iv) simulation with SSI assuming soil behaves non-linearly

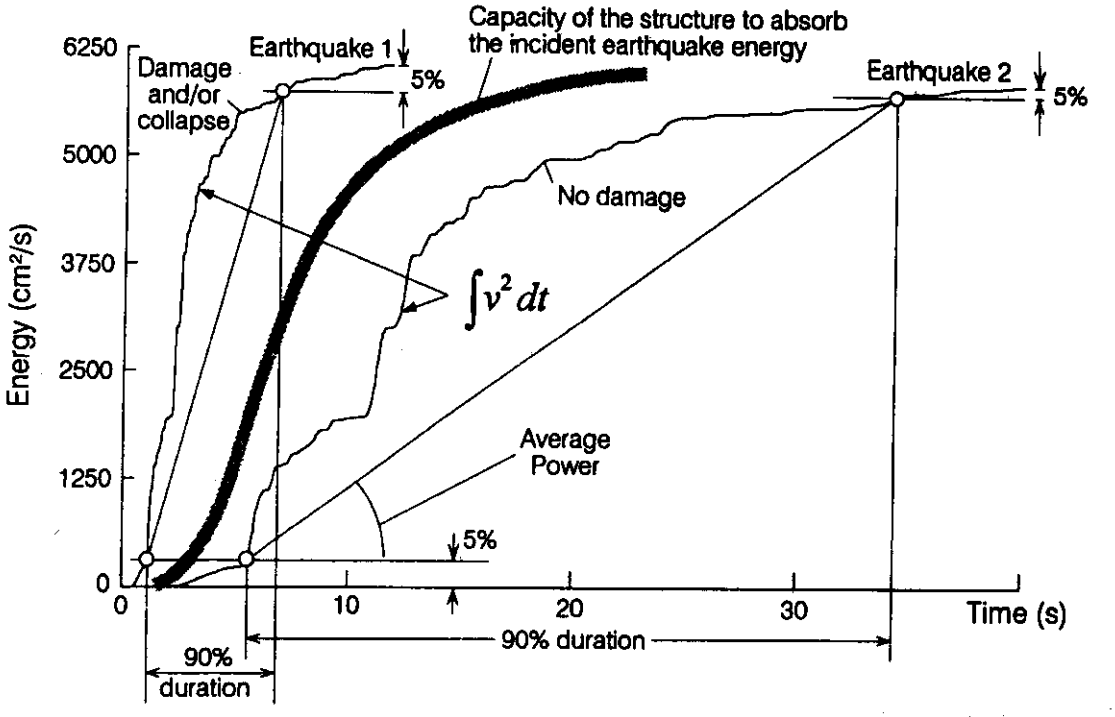

Fig. 22 Comparison of the time histories of two earthquakes that have same input wave energy but different durations, with the energy absorbing capacity of a hypothetical structure

APPENDIX A : POWER DEMAND AND ABSORPTION CAPACITY OF THE STRUCTURE

It is assumed that the velocity pulse entering the structure and deforming it (as shown in Fig. A.1) has amplitude v_b. When the soil-structure interaction can be neglected, $v_b = v_{G,\max}$ ($v_{G,\max}$ is peak velocity of ground motion in the free-field), and when it is present and redistributes the incident wave energy, $v_b = P\,v_{G,\max}$ where $P \leq 1$. Assuming that the soil foundation system has equivalent density ρ_e and shear wave velocity β_e, the energy carried by the incident waves, per unit time and across unit area normal to the direction of propagation, is $\rho_e \beta_e v_b^2$.

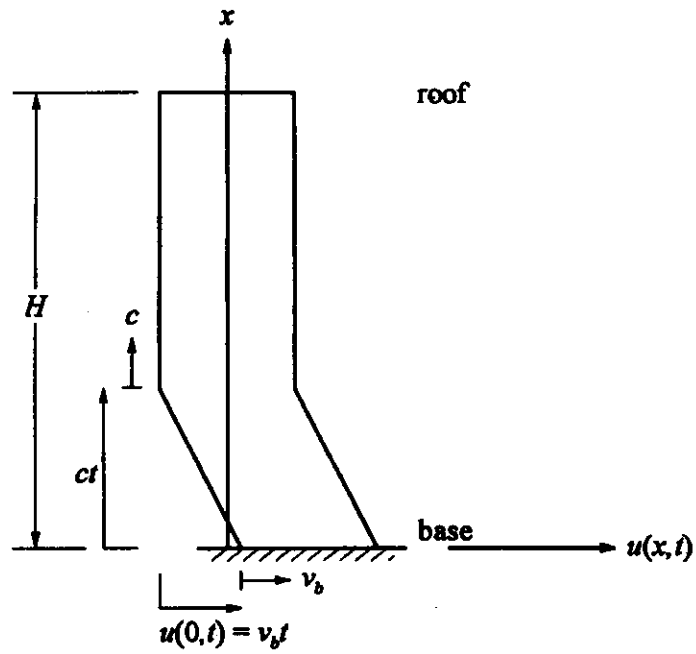

Fig. A.1 Wave caused by sudden movement at the base of the shear building, for constant velocity pulse with amplitude v_b, for time $t < t_0$ (= pulse duration)

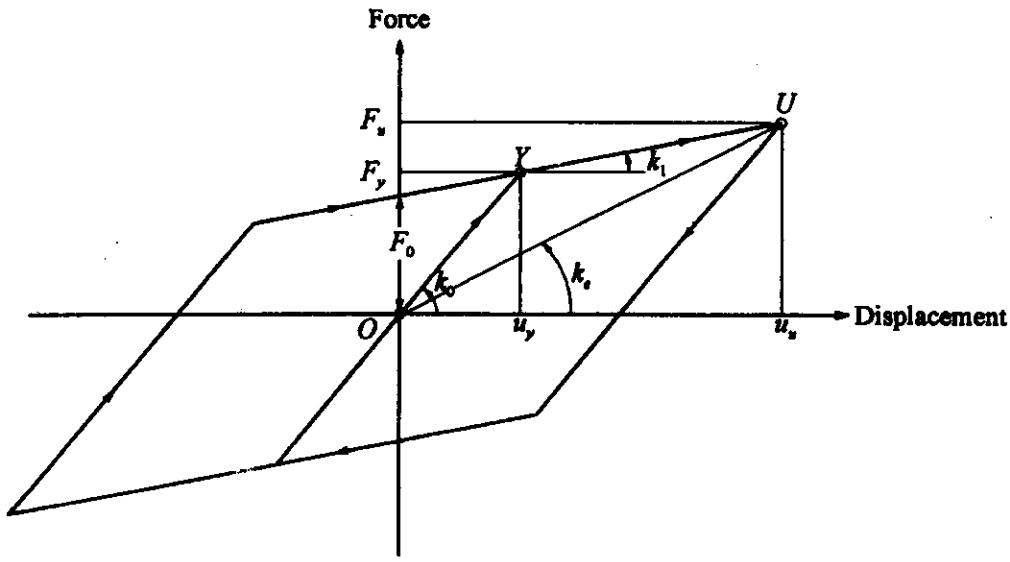

Fig. A.2 Bilinear force-deformation representation of a shear-beam building model experiencing non-linear response

The hysteretic work per one complete cycle of non-linear relative response of the structure is (Figure A.2)

$$W_0 = 4F_0(u_u - u_y) \tag{A.1}$$

Defining $k_0 u_y \equiv F_y = ma_y$, where a_y is the static acceleration which produces deflection u_y, $k_1 = \alpha k_0$, and using the standard definition of ductility, $\mu = u_u/u_y$, one can write

$$W_0 = 4(1-\alpha)\, m_b a_y\, (\mu - 1)/u_y \tag{A.2}$$

By approximating the equivalent stiffness of the non-linear system by the secant modulus (see Figure A.2)

$$k_e = k_0\left[\frac{1+\alpha(\mu-1)}{\mu}\right], \tag{A.3}$$

gives the approximate period of non-linear oscillator $T_e = T_n\xi$ where

$$\xi = \left[\frac{\mu}{1+\alpha(\mu-1)}\right]^{1/2} \tag{A.4}$$

The maximum power, the oscillator can absorb during one cycle of response, is then

$$W_0/T_e = 4(1-\alpha)(\mu-1)m_b a_u\, u_y\, /T_n\, \xi \tag{A.5}$$

and since, for the first mode of vibration $T_n = 4H_{sb}/\beta_b$,

$$W_0/T_e = 4(1-\alpha)(\mu-1)\frac{m_b a_y u_y \beta_b}{4H_{sb}\xi} \tag{A.6}$$

It is not probable that the incident motion will be so regular to allow completion of the complete hysteretic cycle. Instead, the pulse v_b may be one-directional, with low frequency content, and of considerable duration causing monotonic increase in the relative displacement u. Therefore, it is also of interest to examine the relationship of the input power demand relative to the capacity of the structure to absorb this power along the path *OYU* (as shown in Figure A.2). The work accompanying non-linear response in going from *O* to *U* is

$$W_{\rightarrow} = \frac{1}{2}k_0 u_y^2 + (u_u - u_y)k_0 u_y + \frac{1}{2}k_1(u_u - u_y)^2 \tag{A.7}$$

or

$$\begin{aligned} W_{\rightarrow} &= k_0\left[\frac{1}{2} + (\mu-1) + \frac{1}{2}\alpha(\mu-1)^2\right]u_y^2 \\ &= \left[\frac{1}{2} + (\mu-1) + \frac{1}{2}\alpha(\mu-1)^2\right]m_b a_y u_y \end{aligned} \tag{A.8}$$

The time required to reach *U* starting at *O* is approximately $T_e/4$, and this gives the associated power absorbing capacity of the structure

$$4W_{\rightarrow}/T_n\xi = \left[\frac{1}{2} + (\mu-1) + \frac{1}{2}\alpha(\mu-1)^2\right]\frac{m_b a_y u_y 4\beta_b}{4H_{sb}\xi} \tag{A.9}$$

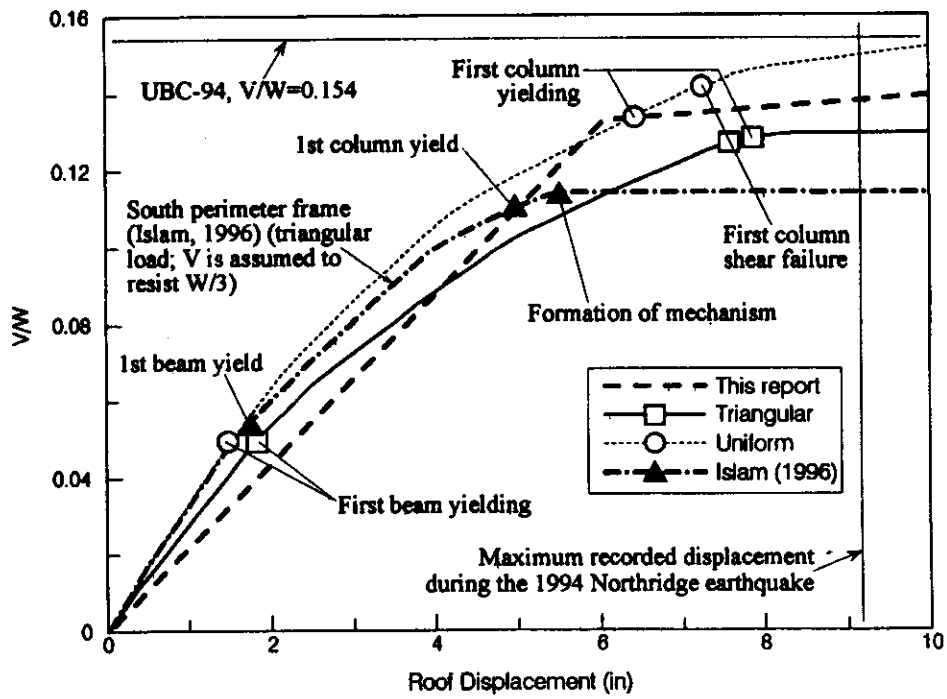

Fig. A.3 Base shear (V) coefficient normalized by 1/3 of the total building weight, W, versus EW roof displacement of VN7SH (after Islam, 1996; and Li and Jirsa, 1998)

For illustration purposes. the values of $a_y = 0.13g$ and $u_y = 15.3$ cm have been estimated based on non-linear static push-over analysis of the EW response of VN7SH building by Islam (1996) and Li and Jirsa (1998). Their results are summarized in Figure A.3, showing the base shear coefficient, V/W, where V is the computed base shear, and W is total weight of the building $\left(W \sim 10^4 \text{ kips}\right)$, plotted versus roof displacement for triangular and uniform load distribution patterns. Also shown in this figure are the "maximum roof displacement" determined by Islam (1996) and by Li and Jirsa (1998) from the recorded data, and the computed UBC-94 base shear $V = 0.154\ W$.

For fixed-base EW response, the two independent estimates of F_y are $F_y = 1300$ kips (5780 kN) (Li and Jirsa, 1998) and $F_y = 1140$ kips (5070 kN) (Islam, 1996). Assuming $u_y = 15.3$ cm, these two estimates imply $F_y u_y = 775$ to 884 kN·m. During 1/4 cycle of the response, and linear deformation in the building, the maximum accumulated potential energy is equal to 387 to 442 kN·m (see Figure A.4, left-top). For $T_n \sim 0.8$ s, we can estimate the largest power of the EW component of the incident waves, which the VN7SH building can take without damage, to be 1932 to 2208 kN·m/s.

The time-dependent evolution of the energy dissipated by non-linear building response will depend on the history of the excitation, but several characteristic milestone values can be estimated *a priori*. This is illustrated in Figure A.4. The shaded area in the top-left of this figure illustrates the largest potential energy in the oscillator, which is still responding in the linear range of response ($u < u_y$), when $\mu = 1$ and when $F = F_y$. For VN7SH building, using static push over analyses of Islam (1996) and Li and Jirsa (1998), for EW response, as indicators of the possible range of F_y, we obtain the estimates of 5070 kN and 5783 kN respectively. A larger and longer lasting incident velocity pulse might force the equivalent oscillator to deform monotonically to, say $u = 2u_y$ ($\mu = 2$), during $T_e/4$. This case is illustrated in the left-bottom part of Figure A.4. Assuming $\alpha = 0.2$ implies the work dissipated by the hysteresis in going from O to Y to U to be 1240 to 1414 kN·m (see Equation (A.8)), and the associated power $4W_{\rightarrow}/T_n\xi$ to be in the range from 4816 to 5492 kN·m/s. The right part of Fig. A.4 shows the closed hysteretic loop, starting at OYU and returning to Y after one complete cycle lasting $T_n\xi$ seconds. The work dissipated by such a loop, assuming F_y as above, with $\mu = 2$ and $\alpha = 0.2$ is 2480 to 2829 kN·m. The corresponding maximum

power this oscillator can dissipate along this path is then 2407 to 2746 kN·m/s. These estimates of the building capacity to absorb energy and power are shown by the gray bands in Figure 21a.

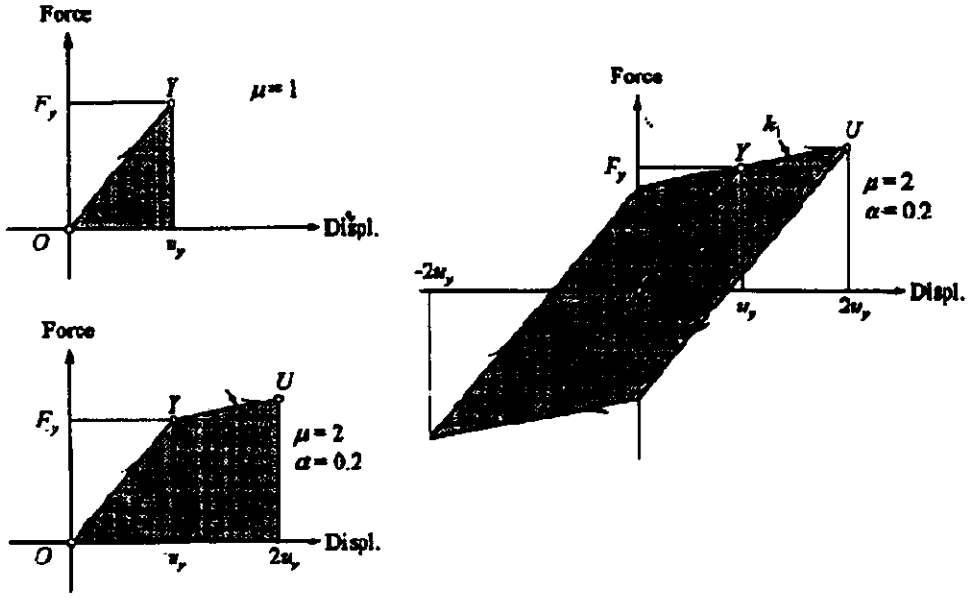

Fig. A.4 The shaded areas represent: (left-top) maximum potential energy associated with linear response; (left-bottom) hysteretic energy associated with monotonic non-linear response; and (right) hysteretic energy associated with oscillatory (periodic, one cycle) excitation

REFERENCES

1. Akiyama, H. (1985). "Earthquake-Resistant Limit-State Design for Buildings", Univ. of Tokyo Press, Tokyo, Japan.
2. Akiyama, H. (1988). "Earthquake Resistant Design Based on the Energy Concept", Proc. of the Ninth World Conference on Earthquake Engg., Tokyo, Japan, pp. 905-910.
3. Akiyama, H. (1997). "Damage-Controlled Earthquake Resistant Design Method Based on the Energy Concept", in Report UCB/EERC-97/05, Earthquake Engineering Research Center, University of California, Berkeley, California, U.S.A., pp. 49-56.
4. Anderson, J.C. and Bertero, V.V. (1969). "Seismic Behavior of Multistory Frames by Different Philosophies", Report UCB/EERC-69/11, Earthquake Engineering Research Center, University of California, Berkeley, California, U.S.A..
5. Arias, A. (1970). "A Measure of Earthquake Intensity", in Seismic Design of Nuclear Power Plants (ed. R.J. Hansen), The Mass. Inst. of Tech. Press, U.S.A.
6. Benioff, H. (1934). "The Physical Evaluation of Seismic Destructiveness", Bull. Seism. Soc. Amer., Vol. 24, pp. 398-403.
7. Biot, M.A. (1932). "Vibrations of Buildings during Earthquake", Chapter II in Ph.D. thesis No. 259 entitled "Transient Oscillations in Elastic Systems", Aeronautic Dept., Calif. Inst. Of Tech., Pasadena, California, U.S.A.
8. Biot, M.A. (1933). "Theory of Elastic Systems Vibrating under Transient Impulse with an Application to Earthquake–Proof Buildings", Proc. National Academy of Science, Vol. 19, No. 2, pp. 262-268.
9. Biot, M.A. (1934). "Theory of Vibration of Buildings during Earthquake", Zeitschrift für Angewandte Matematik and Mechanik, Vol. 14, No. 5, pp. 213-223.
10. Biot, M.A. (1941). "A Mechanical Analyzer for the Prediction of Earthquake Stresses", Bull. Seism. Soc. Amer., Vol. 31, No. 2, pp. 151-171.

11. Biot, M.A. (1942). "Analytical and Experimental Methods in Engineering Seismology", ASCE Transactions, Vol. 108, pp. 365-408.
12. Blume, J.A. (1960). "A Reserve Energy Technique for the Earthquake Design and Rating of Structures in the Inelastic Range", Proc. of the Second World Conference on Earthquake Engg., Tokyo, Japan, pp. 1061-1083.
13. Decanini, L.D. and Mollaioli, F. (2001). "An Energy-Based Methodology for the Assessment of Seismic Demand", Soil Dyn. and Earthquake Engg., Vol. 21, No. 2, pp. 113-137.
14. Duncan, W.J. (1952). "A Critical Examination of the Representation of Massive and Elastic Bodies by Systems of Rigid Masses Elastically Connected", Quart. J. Mech. Appl. Math., Vol. 5, No. 1, pp. 97-108.
15. Fajfar, P. and Fischinger, M.A. (1990). "A Seismic Design Procedure including Energy Concept", Proc. of the Ninth European Conference on Earthquake Engg., Moscow, USSR.
16. Gutenberg, B. and Richter, C.F. (1956). "Earthquake Magnitude, Intensity, Energy, and Acceleration", Bull. Seism. Soc. Amer., Vol. 46, No. 2, pp. 105-145.
17. Hao, T.-Y. (2002). "Investigation of Energy Flow in Earthquake Response of Structures", Ph.D. Thesis, Dept. of Civil Engrg., Univ. of Southern California, Los Angeles, California, U.S.A..
18. Hayir, A., Todorovska, M.I. and Trifunac, M.D. (2001). "Antiplane Response of a Dike with Flexible Soil-Structure Interaction to Incident SH-Waves", Soil Dyn. and Earthquake Engg., Vol. 21, No. 7, pp. 603-613.
19. Housner, G.W. (1956). "Limit Design of Structures to Resist Earthquakes", Proc. of the First World Conference on Earthquake Engg., Berkeley, California, pp. 5.1-5.13.
20. Husid, R. (1967). "Gravity Effects on the Earthquake Response of Yielding Structures", Ph.D. Thesis, Calif. Inst. of Tech., Pasadena, California, U.S.A.
21. Iguchi, M. and Luco, J.E. (1982). "Vibration of Flexible Plate on Viscoelastic Medium", J. of Engg. Mech., ASCE, Vol. 108, No. 6, pp. 1103-1120.
22. Islam, M.S. (1996). "Analysis of the Response of an Instrumented 7-story Nonductile Concrete Frame Building Damaged during the Northridge Earthquake", Professional Paper 96-9, Los Angeles Tall Buildings Structural Design Council.
23. Ivanović, S.S., Trifunac, M.D., Novikova, E.I., Gladkov, A.A. and Todorovska, M.I. (1999). "Instrumented 7-story Reinforced Concrete Building in Van Nuys, California: Ambient Vibration Surveys Following the Damage from the 1994 Northridge Earthquake", Report CE 99-03, Dept. of Civil Eng., Univ. of Southern California, Los Angeles, California, U.S.A.
24. Ivanović, S.S., Trifunac, M.D., Novikova, E.I., Gladkov, A.A. and Todorovska, M.I. (2000). "Ambient Vibration Tests of a Seven-Story Reinforced Concrete Building in Van Nuys, California, Damaged by the 1994 Northridge Earthquake", Soil Dyn. and Earthquake Engg., Vol. 19, No. 6, pp. 391-411.
25. Joyner, W.B. (1975). "A Method for Calculating Nonlinear Seismic Response in Two Dimensions", Bull. Seism. Soc. Amer., Vol. 65, No. 5, pp. 1337-1357.
26. Joyner, W.B. and Chen, A.T.F. (1975). "Calculating of Nonlinear Ground Response in Earthquakes", Bull. Seism. Soc. Amer., Vol. 65, No. 5, pp. 1315-1336.
27. Lee, V.W. (1979). "Investigation of Three-Dimensional Soil-Structure Interaction", Report CE 79-11, Dept. of Civil Eng., University of Southern California, Los Angeles, California, U.S.A..
28. Li, R.Y. and Jirsa, J.D. (1998). "Nonlinear Analysis of an Instrumented Structure Damaged in the 1994 Northridge Earthquake", Earthquake Spectra, Vol. 14, No. 2, pp. 265-283.
29. Liou, G.-S. and Huang, P.R. (1994). "Effects of Flexibility on Impedance Functions for Circular Foundations", J. of Engg. Mech., ASCE, Vol. 120, No. 7, pp. 1429-1446.
30. Luco, J.E., Trifunac, M.D. and Wong, H.L. (1986). "Soil Structure Interaction Effects on Forced Vibration Tests", Report 86-05, Dept. of Civil Eng., Univ. of Southern California, Los Angeles, California, U.S.A.
31. Papageorgiou, A.S. and Lin, B.C. (1991). "Analysis of Recorded Earthquake Response and Identification of a Multi-story Structure Accounting for Foundation Interaction Effects", Soil Dyn. and Earthquake Engg., Vol. 10, No. 1, pp. 55-64.

32. Richart, F.E., Jr., Hall, J.R., Jr. and Woods, R.D. (1970). "Vibrations of Soils and Foundations", Prentice-Hall, Englewood Cliffs, New Jersey, U.S.A.

33. Rodrigues, M.E. and Montes, R. (2000). "Seismic Response and Damage Analysis of Buildings Supported on Flexible Soils", Earthquake Engg. and Structural Dynamics, Vol. 29, No. 5, pp. 647-665.

34. Sezawa, K. and Kanai, K. (1936). "Improved Theory of Energy Dissipation in Seismic Vibrations on a Structure", Bull. Earth. Res. Inst., Vol. XIV, Part 2, pp. 164-168.

35. Tanabashi, R. (1937). "On the Resistance of Structures to Earthquake Shocks", Memoirs of the College of Engineering, Kyoto Imperial University, Japan.

36. Tanabashi, R. (1956). "Studies of the Nonlinear Vibrations of Structures Subjected to Destructive Earthquakes", Proc. of the First World Conference on Earthquake Engg., Berkeley, California, U.S.A.

37. Tembulkar, J.M. and Nau, J.M. (1987). "Inelastic Modeling and Seismic Energy Dissipation", J. of Struct. Engg., ASCE, Vol. 113, No. 6, pp. 1373-1377.

38. Todorovska, M.I. and Trifunac, M.D. (1990a). "A Note on the Propagation of Earthquake Waves in Buildings with Soft First Floor", J. of Engg. Mech., ASCE, Vol. 116, No. 4, pp. 892-900.

39. Todorovska, M.I. and Trifunac, M.D. (1990b). "A Note on Excitation of Long Structures by Ground Waves", J. of Engg Mech., ASCE, Vol. 116, No. 4, pp. 952-964.

40. Todorovska, M.I. and Trifunac, M.D. (1990c). "Analytical Model for In-plane Building-Foundation-Soil Interaction: Incident P-, SV- and Rayleigh Waves", Report 90-01, Dept. of Civil Engg., Univ. of Southern California, Los Angeles, California, U.S.A..

41. Todorovska, M.I. and Trifunac, M.D. (1991). "Radiation Damping during Two-Dimensional Building-Soil Interaction", Report 91-01, Dept. of Civil Eng., Univ. of Southern California, Los Angeles, California, U.S.A.

42. Todorovska, M.I. and Trifunac, M.D. (1992). "The System Damping, the System Frequency and the System Response Peak Amplitudes during In-plane Building-Soil Interaction", Earthquake Eng. and Struct. Dyn., Vol. 21, No. 2, pp. 127-144.

43. Todorovska, M.I. and Trifunac, M.D. (1993). "The Effects of Wave Passage on the Response of Base-Isolated Buildings on Rigid Embedded Foundations", Report CE 93-10, Dept of Civil Eng., Univ. of Southern California, Los Angeles, California, U.S.A.

44. Todorovska, M.I., Ivanović, S.S. and Trifunac, M.D. (2001a). "Wave Propagation in a Seven-Story Reinforced Concrete Building, I: Theoretical Models", Soil Dyn. and Earthquake Engg., Vol. 21, No. 3, pp. 211-223.

45. Todorovska, M.I., Ivanović, S.S. and Trifunac, M.D. (2001b). "Wave Propagation in a Seven-Story Reinforced Concrete Building, II: Observed Wave Numbers", Soil Dyn. and Earthquake Engg., Vol. 21, No. 3, pp. 225-236.

46. Todorovska, M.I., Hayir, A. and Trifunac, M.D. (2001c). "Antiplane Response of a Dike on Flexible Embedded Foundation to Incident SH-Waves", Soil Dyn. and Earthquake Engg., Vol. 21, No. 7, pp. 593-601.

47. Trifunac, M.D. (1994). "Q and High Frequency Strong Motion Spectra", Soil Dyn. and Earthquake Engg., Vol. 13, No. 3, pp. 149-161.

48. Trifunac, M.D. (1995). "Empirical Criteria for Liquefaction of Sands via Standard Penetration Tests and Seismic Wave Energy", Soil Dyn. and Earthquake Engg., Vol. 14, No. 4, pp. 419-426.

49. Trifunac, M.D. (1997). "Differential Earthquake Motion of Building Foundation", J. of Struct. Engg., ASCE, Vol. 123, No. 4, pp. 414-422.

50. Trifunac, M.D. and Brady, A.G. (1975). "A Study of the Duration of Strong Earthquake Ground Motion", Bull. Seism. Soc. Amer., Vol. 65, pp. 581-626.

51. Trifunac, M.D. and Hao, T.-Y. (2001). "7-Story Reinforced Concrete Building in Van Nuys, California: Photographs of the Damage from the 1994 Northridge Earthquake", Report CE 01-05, Dept. of Civil Engrg., Univ. of Southern California, Los Angeles, California, U.S.A.

52. Trifunac, M.D. and Todorovska, M.I. (1996). "Nonlinear Soil Response – 1994 Northridge California Earthquake", J. Geotechnical Engg., ASCE, Vol. 122, No. 9, pp. 725-735.

53. Trifunac, M.D. and Todorovska, M.I. (1997a). "Northridge, California, Earthquake of January 17, 1994: Density of Red-Tagged Buildings versus Peak Horizontal Velocity and Site Intensity of Strong Motion", Soil Dyn. and Earthquake Engg., Vol. 16, No. 3, pp. 209-222.

54. Trifunac, M.D. and Todorovska, M.I. (1997b). "Northridge, California, Earthquake of January 17, 1994: Density of Pipe Breaks and Surface Strains", Soil Dyn. and Earthquake Engg., Vol. 16, No. 3, pp. 193-207.

55. Trifunac, M.D. and Todorovska, M.I. (1997c). "Response Spectra for Differential Motion of Columns", Earthquake Engg. and Struct. Dyn., Vol. 26, No. 2, pp. 251-268.

56. Trifunac, M.D. and Todorovska, M.I. (1998a). "Nonlinear Soil Response as a Natural Passive Isolation Mechanism – The 1994 Northridge, California Earthquake", Soil Dynamics and Earthquake Eng., Vol. 17, No. 1, pp. 41-51.

57. Trifunac, M.D. and Todorovska, M.I. (1998b). "The Northridge, California, Earthquake of 1994: Fire Ignition by Strong Shaking", Soil Dyn. and Earthquake Engg., Vol. 17, No. 3, pp. 165-175.

58. Trifunac, M.D. and Todorovska, M.I. (1998c). "Damage Distribution during the 1994 Northridge, California, Earthquake Relative to Generalized Categories of Surficial Geology", Soil Dyn. and Earthquake Engg., Vol. 17, No. 7, pp. 239-253.

59. Trifunac, M.D. and Todorovska, M.I. (1998d). "Amplification of Strong Ground Motion and Damage Patterns during the 1994 Northridge, California, Earthquake", Proc. ASCE Specialty Conf. on Geotechnical Earthquake Engg. and Soil Dyn., Seattle, Washington, Geotechnical Special Publ. No. 75, ASCE, Vol. I, pp. 714-725.

60. Trifunac, M.D. and Todorovska, M.I. (1999). "Reduction of Structural Damage by Nonlinear Soil Response", J. Structural Engrg., ASCE, Vol. 125, No. 1, pp. 89-97.

61. Trifunac, M.D. and Todorovska, M.I. (2001a). "Evolution of Accelerographs, Data Processing, Strong Motion Arrays and Amplitude and Spatial Resolution in Recording Strong Earthquake Motion", Soil Dyn. and Earthquake Engg., Vol. 21, No. 6, pp. 537-555.

62. Trifunac, M.D. and Todorovska, M.I. (2001b). "Recording and Interpreting Earthquake Response of Full-Scale Structures", in Proc. NATO Workshop on Strong Motion Instrumentation for Civil Engineering Structures (eds. M. Erdik et al.), Kluwer Academic Publishers, pp. 131-155.

63. Trifunac, M.D., Ivanović, S.S., Todorovska, M.I., Novikova, E.I. and Gladkov, A.A. (1999a). "Experimental Evidence for Flexibility of a Building Foundation Supported by Concrete Friction Piles", Soil Dyn. and Earthquake Engg., Vol. 18, No. 3, pp. 169-187.

64. Trifunac, M.D., Ivanović, S.S. and Todorovska, M.I. (1999b). "Seven Story Reinforced Concrete Building in Van Nuys, California: Strong Motion Data Recorded between 7 February 1971 and 9 December 1994, and Description of Damage Following Northridge, 17 January 1994 Earthquake", Report 99-02, Dept. of Civil Eng., Univ. of Southern California, Los Angeles, California, U.S.A.

65. Trifunac, M.D., Ivanović, S.S. and Todorovska, M.I. (2001a). "Apparent Periods of a Building, Part I: Fourier Analysis", J. of Struct. Engg., ASCE, Vol. 127, No. 5, pp. 517-526.

66. Trifunac, M.D., Ivanović, S.S. and Todorovska, M.I. (2001b). "Apparent Periods of a Building, Part II: Time-Frequency Analysis", J. of Struct. Engg., ASCE, Vol. 127, No. 5, pp. 527-537.

67. Trifunac, M.D., Todorovska, M.I. and Hao, T.-Y. (2001c). "Full-Scale Experimental Studies of Soil-Structure Interaction – A Review", Proc. 2nd U.S.-Japan Workshop on Soil-Structure Interaction, Tsukuba City, Japan.

68. Trifunac, M.D., Ivanović, S.S. and Todorovska, M.I. (2001d). "Wave Propagation in a Seven-Story Reinforced Concrete Building, III: Damage Detection via Changes in Wave Numbers", Soil Dyn. and Earthquake Engrg. (in press).

69. Trifunac, M.D., Hao, T.-Y. and Todorovska, M.I. (2001e). "Response of a 14-Story Reinforced Concrete Structure to Nine Earthquakes: 61 Years of Observation in the Hollywood Storage Building", Report 01-02, Dept. of Civil Eng., Univ. of Southern California, Los Angeles, California, U.S.A.

70. Trifunac, M.D., Hao, T.-Y. and Todorovska, M.I. (2001f). "On Energy Flow in Earthquake Response", Report 01-03, Dept. of Civil Eng., Univ. of Southern California, Los Angeles, California, U.S.A.

71. Uang, C.M. and Bertero, V.V. (1988) "Use of Energy as a Design Criterion in Earthquake-Resistant Design", Report UCB/EERC-88/18, Earthquake Engineering Research Center, Univ. of California, Berkeley, California, U.S.A.

72. Uang, C.M. and Bertero, V.V. (1990). "Evaluation of Seismic Energy in Structures", Earthquake Engg. and Struct. Dyn., Vol. 19, No. 1, pp. 77-90.

73. Zahrah, T.F. and Hall, W.J. (1984). "Earthquake Energy Absorption in SDOF Structures", J. of Struct. Engg., Vol. 110, No. 8, pp. 1757-1772.